Aalto-yliopisto
Aalto-universitetet
Aalto University

Master's Programme in Building Technology

Ground-penetrating radar (GPR) for non-destructive characterization of reinforced concrete structures

Muhammad Haseeb Latif

Master's Thesis
2022

Author Muhammad Haseeb Latif

Title of thesis Ground-penetrating radar (GPR) for non-destructive characterization of reinforced concrete structures

Programme Building Technology

Major Concrete structures

Thesis supervisor Prof. Jouni Punkki

Thesis advisor(s) Dr. Fahim Al Nashawy, Staff Scientist

Date 29.12.2022 **Number of pages** 90+0 **Language** English

Abstract

Characterizing reinforced concrete structures is an overall evaluation process, including inspection, investigation, and testing of the concrete structures. To investigate existing concrete structures in service is preferred to use non-destructive techniques. For non-destructive investigation of reinforced concrete structures, Ground Penetrating radar (GPR) is a preferred instrument and is worldwide accepted for its ability to detect defects and provision of reliable images of the substructure of concrete structures. Ground penetrating radar (GPR) emits electromagnetic energy waves into the surface of concrete due to encounters with materials having different dielectric constants; waves deflect back and make the display of substructure on radargram.

This thesis work is aimed to find the location of different types of construction defects, foreign objects, and reinforcement details in concrete structures. For this purpose, PS 1000 X-SCAN CONCRETE SCANNER is used to obtain image scans from the thick concrete testing wall, retaining wall and precast RC slabs. GPR scans are analysed using Profis Detection Software by HILTI to get the required results.

Detection and location of construction defects, rebar mapping, concrete cover depth and location of other anomalies and metal objects in the substructure of concrete are beneficial for the maintenance and repair of concrete structures. The service life of concrete structures can be predicted from GPR scanning results using the evaluation of defects leading to failure of the concrete structures.

Keywords Characterization, Non-Destructive Testing, Ground Penetrating Radar, Electromagnetic Waves, Foreign Objects, Image Scans

Contents

Preface

This thesis work was a part of master's degree Programme in Building Technology at Aalto University, School of Engineering. In this study, three concrete structures are inspected using GPR system to characterize the concrete structures.

I would like to express my deepest gratitude to my supervisor Professor of Practice Jouni Punkki for awarding me this opportunity to work on GPR technology. I would also like to extend my deepest acknowledgement to Dr. Fahim Al Neshawy, Staff Scientist for his help, & support throughout the different phases of planning, methodology, experimenting, compiling results, formulating analysis, & thesis writing. I would like to thank my best friend in Finland Osama bin Shafaat who helped me in every aspect of life and gave me a motivational company to write this thesis.

Otaniemi, 29 December 2022
Haseeb Latif

Symbols and abbreviations

Symbols

ε	Complex permittivity or dielectric constant
ε'	Real part of complex permittivity
ε''	Imaginary part of complex permittivity
ε_0	Dielectric constant of vacuum or air (8.85∗10−12 farad/meter)
ε_r	Relative dielectric constant
$\mathbf{v}_\mathbf{m}$	Velocity of EM waves
C	Speed of Light

Abbreviations

GPR	Ground Penetrating Radar
EM	Electro Magnetic Waves
NDT	Non-Destructive Techniques
RC	Reinforced Concrete
CW -GPR	Continuous Wave GPR system
SF-GPR	Stepped Frequency GPR system
WARR	Wide Angle Reflection method
RDP	Relative Dielectric Permittivity

List of Figures

List of Tables

1 Introduction

Concrete structures have vital importance in civil infrastructure as concrete materials are easily and locally available. Concrete has the property to be moulded in any desired shape and it is aesthetically demanded everywhere in all over the world. Reinforced concrete structures are potentially durable and able to withstand to various worst and adverse environmental conditions (Saraswathy, 2007). However, failures occur in concrete structures due to various factors including construction defects, internal defects, chemical attack, and mechanical damages etc. Modern infrastructures are mostly made of concrete including bridges, dams, viaducts, buildings, and tunnels need periodic maintenance to be functional and serving their main purpose (Naotoshi YasudaNorikazu, 2020). It is natural rule that a problem needs to be detected first to be solved. Inspection of these structures includes the detection of the problems using different mechanical and digital methods.

Common methods to investigate the structures are destructive and involves physical testing, sampling to evaluate structural and mechanical characteristics. On the other hand, Non-Destructive Testing (NDT) is an effective way of investigating the existing structures with high resolution, low time and cost effective and this resulted in the development of several NDT's techniques for monitoring civil infrastructures, accurate analysis of physical parameters to characterize the structures. GPR has been used for detection of location of reinforcement, air voids, construction defects (honeycombs) and buried or embedded objects in the subsurface of concrete structures.

Ground Penetrating Radar (GPR) is a non-destructive testing technique to find the hidden objects and the location of buried objects in civil engineering structures (Tahar Bachiri, 2022). It is vastly used in the evaluation of concrete structures and the characterization of existing structures. Structures need to be renovated and having not the technical documents and details, using GPR we can assess the current condition of reinforcements and rebars location and amount of rebars to be restored. The initial use of GPR was in geophysics to explore ground properties and then it was used in civil engineering, an inspection of hard ground surfaces, and cavities detection at airports (K. Agred, 2018). Later radar technique was used in the detection of voids in masonry structures, delamination in concrete bridge decks, location of pipes, thicknesses of the concrete slab and roads, the concrete cover of concrete structures, determination of moisture content in concrete and location of reinforcement in concrete structures.

1.1 Problem statement

According to (K. Agred, 2018) concrete cover is vital important in the protection of concrete elements especially reinforcement as concrete cover is the only barrier against carbon dioxide and chloride penetration to protect reinforcement from corrosion and takes responsibility in the durability of concrete element. Most important factor is thickness of concrete cover resistant to carbonation and chloride intrusion and thickness of concrete cover must be in accordance with the depth of carbonation and chloride intrusion, these are most relevant parameters to reinforcement corrosion. Measurement of concrete cover thickness using destructive techniques is difficult and slow which is not feasible for the mega structure's evaluation. For this purpose, NDT (Non-destructive Techniques) are favourable to use and GPR (Ground Penetrating Radar) is highly recommended to measure the concrete cover thickness.

Internal defects and cracks are vital to be detected as they increase the structure's vulnerability to failure. Mostly in tunnels external defects and leakages can be observed directly but internal defects like voids, lining-rock separation, water seepage and other structural defects are difficult to observe and investigate. These defects are critical to identify, locate and classify for the maintenance and safety of the tunnels (Senlin Yang, 2021). Using non-destructive testing techniques (NDT) like infrared thermography, multispectral analysis, ultrasonic pulses, and GPR (Ground penetrating radar). GPR is preferred due to its fast detection speed, excellent penetrating ability, portability, and convenience.

Using GPR (Ground Penetrating Radar) different existing concrete structures are analysed in this thesis to find the reinforcement location, internal defects like cavities and cracks, concrete cover, and hidden objects in the concrete structure under examination. Concrete structures analysed in this thesis are a thick mock wall, a retaining wall, and prestressed slabs.

1.2 Thesis aims and methods

This thesis is aimed to find location of reinforcement, concrete cover thickness, location of hidden objects, detection of construction defects and other anomalies in the subsurface of reinforced concrete structures.
To achieve this goal, three different concrete structural elements (Thick Mock Wall, Retaining Wall, and precast concrete slabs are scanned using GPR 1000X Concrete scanner with image scan technique. These image scans are processed and analysed using a digital tool named Hilti Profis Detection.

1.3 Thesis scope

This thesis is limited to determine concrete cover of the structural elements, location of reinforcement, finding internal cracks and cavities, and finding the targeted hidden and buried objects in the concrete structures using GPR scanner. There is not destructive testing and data is used, only GPR scans are used to obtain the data to determine the thesis objectives.

1.4 Thesis outline

Rest of the thesis is divided into five chapters. Chapter 2 includes the literature re-view, construction defects in concrete structures, GRP instrumentation, reviews different NDT methodologies to detect the defects and problems in the existing concrete structures, description of defects can be detected using GPR and deterioration phases of concrete structures. Chapter 3 explains the methodology and GPR measurements taken from three different experimental sites and objects. In chapter 4 results and analysis of the GPR investigation are discussed briefly with visual explanations of GPR scans. Chapter 5 summarises and conclude the thesis work and provides the future aspects of the research work on GPR investigations of concrete structures.

2 Literature review – GPR applications in concrete structures

This chapter is divided into three major parts. The first part introduces the Ground Penetrating Radar (GPR) electromagnetic concept, components, scanning system and data processing. The second part reviews the construction defects in the civil infrastructure and what type of defects can be detected or investigated using GPR. In second part deterioration damages to reinforced concrete structure and the main causes of deterioration are described. The third part includes the concrete characterization using GPR and GPR methodology along with GPR applications in the Civil engineering.

2.1 Ground Penetrating Radar – GPR

GPR (Ground Penetrating Radar) is non-destructive and non-invasive imaging technique used worldwide for the inspection and investigation of defects in geological and civil infrastructures (Yelf & Yelf, n.d.). GPR is imaging method that provides the high-resolution view in the form of images, scans with the visualization of defects, buried objects and other construction defects. It won't be wrong to say that currently GPR is most effective, versatile, and robust tool for subsurface investigation of civil infrastructure (Salucci et al., 2017). First use of GPR was done in Antarctica for ice sounding in 1970 and now it gained the worldwide acceptance in inspection and investigation purposes. For multi-inspection tasks like detection of buried objects like pipes and cables, investigation of layering of roads and railway ballast, detailed mapping of steel reinforcement in concrete structures.

2.1.1 Concrete scanner – GPR principles

GPR working principle is based on radar where source transmits the electromagnetic waves in varying frequency range of 10 MHz to 4 GHz into the object under experiment. In other words, GPR emits pulses of electromagnetic energy in the subsurface and when it encounters with objects having different dielectric constants, some of energy reflect and leaves a display on radargram. These electromagnetic waves travel through the media of the material to the ultimate attenuation of the signals. When a physical continuity or any object is encountered EM waves partially reflect to the receiver to showing the features or premature picture of the hidden objects in the subsurface(Tosti et al., 2020).

According to (Yelf & Yelf, n.d.) there are two different types of GPR systems are in the market based on the types of transmitted signals (1) Impulse radar system (2) Continuous Wave GPR (CW-GPR) System. In impulse radar system short duration wide band radio energy is transmitted in the form of

multiple small pulses in the range of 50000/second to 100000/seconds. Impulse GPR system is economical, easily manufactured, widely used with transmission of limited mean signal power. (L. Liu & Fang, 2010) says that impulse radar system is very attractive and famous due to its high-resolution applications and simple manufactured system. Advantages of the Impulse system radar are high resolution, deeper penetration depths due to narrowest pulse duration. Continuous Wave GPR system works on sinusoidal radio waves of single frequency, and it is not so commonly used system. In this category there is another Step Frequency GPR (SF-GPR) system in which multiple steps of discrete frequencies of radio energy are used and programmed in a stepwise fashion. In both CW systems more mean power can be transmitted although higher level of signal processing is used to covert the raw data into interpretable form. Difference between both GPR systems can be seen form *Figure 1*.

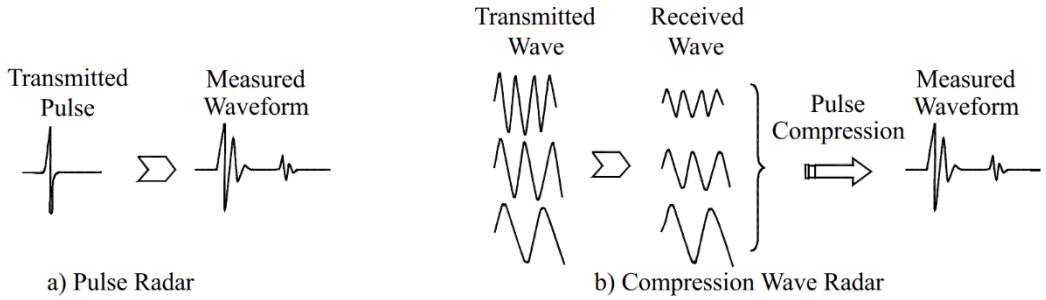

Figure 1- Schematic Diagrams of Pulse Radar and Continuous Wave Radar(Yelf & Yelf, n.d.).

There are two modes can be used in the GPR, reflection and transmission modes. In reflection mode transmitted energy into the material is processed after reflecting from the material due to difference of dielectric constant. Reflection Profiling survey method is commonly used and processed using two antennas like transmitter (Tx) to transmit the energy pulses in the material and a receiver (Rx) to receive back the reflected energy. This is also called bistatic mode and both antennas are shown in. To achieve higher frequency both antennas are combined in one box called transducer.

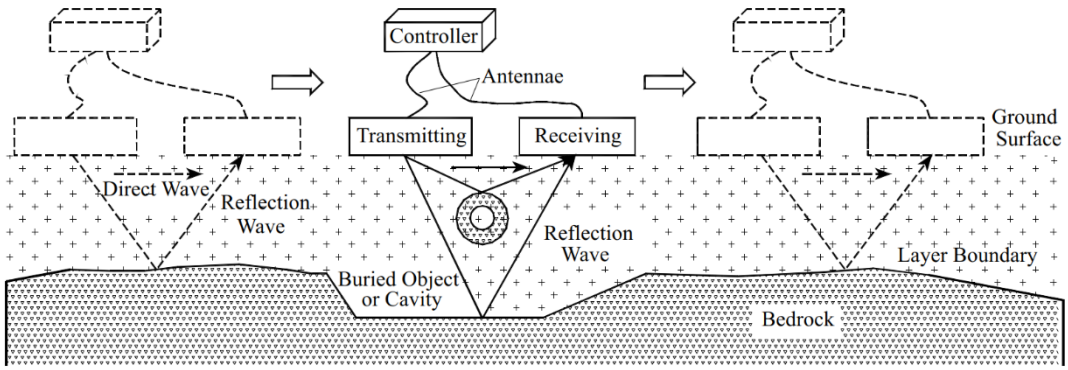

Figure 2- Measurement of a 2D GPR Profile using constant-offset Tx and Rx antennae.(Yelf & Yelf, n.d.)

Figure 2 shows the controller and two antennas, controller amplify and display the reflected energy (waves /signals) from the subsurface objects. Due to difference of dielectric properties of the medium material reflection of signals takes place. Subsurface velocity information can be obtained using Wide Angle Reflection method (WARR) by separating the antennas progressively from each other and a delay can be recorded in the arrival of the signals as shown in *Figure 3*.

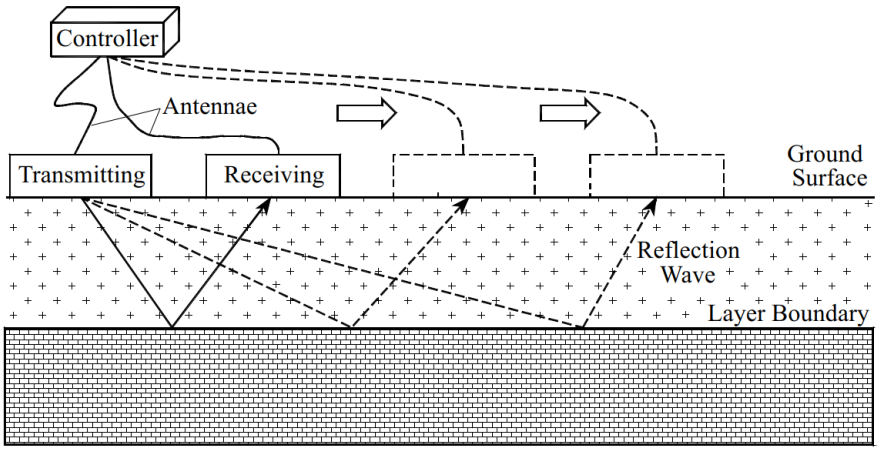

Figure 3- Wide Angle Velocity Measurement.(Yelf & Yelf, n.d.)

There is another method of GPR is called Borehole radar system in which waterproof antennas are placed in the boreholes suspended by wires connected to a system. Boreholes kept uncased or with PVC casing as metal casing interrupt the GPR working in the boreholes. In single borehole both transmitter and receiver are inserted with a specified separation between antennas the reflection profile of EM waves produced from surrounding is obtained. In case of more than one borehole BH, transmission mode is used to get the reflection profile and for transmission measurements position of transmitter is fixed in one borehole and receiver is moved in the other borehole with repetitions for provision of full ray path tomographic coverage of the intermediate rock as shown in the *Figure 4*. (Yochim et al., 2013) used borehole GPR system for the estimation of water content in active landfill. Since basic principle of the GPR is to send the electromagnetic waves through material and some electromagnetic energy waves come back to the receiver due to difference of dielectric properties of anomalies in the medium (Concrete material). Reflected energy comes back to the receiver and generates the signal proportional to the amplitude of the reflected electromagnetic energy(*Guidebook on Non-Destructive Testing of Concrete Structures*, n.d.). Magnitude of the reflected energy depends on the dielectric constant difference, where it will be higher reflected energy will be reflected high and vice versa depending on the type of the material of the anomalies.

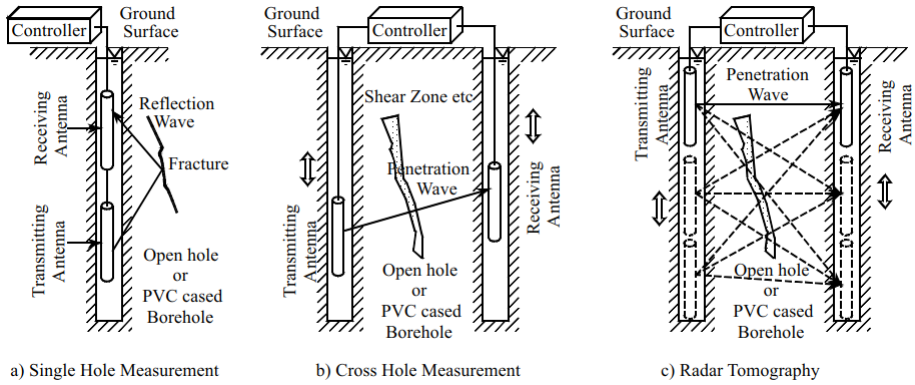

Figure 4- Measurement Variations with Borehole Radar.(Yelf & Yelf, n.d.)

2.1.2 Dielectric materials properties and why it matters to GPR?

A material which conducts the electromagnetic energy is called dielectric material and ability of that material to store a charge from electromagnetic field and release the energy is called dielectric constant of the material. It is also called relative dielectric permittivity (RDP), varies for different geological materials, and affects the velocity of GPR signals. RDP encounters both electromagnetic and electrical properties of the medium. Most important factor is the direct relation to velocity of electromagnetic waves of GPR (*What Is a Trace? - Guideline Geo*, n.d.).

Two properties critically important to dielectric materials are real and imaginary parts of the dielectric permittivity of the material, following equation show the relation between these two complex parts(*Guidebook on Non-Destructive Testing of Concrete Structures*, n.d.).

$$\varepsilon = \varepsilon' - i\varepsilon''$$

ε = complex permittivity or dielectric constant
ε' = real part of complex permittivity
ε'' = imaginary part of complex permittivity

In general dielectric constant is described in dimensionless form by dividing it with the dielectric constant of vacuum and it is then called relative dielectric constant or relative dielectric permittivity of the material.

$$\boldsymbol{\varepsilon r = \frac{\varepsilon}{\varepsilon 0}}$$

Where:
ε = dielectric constant (farad/meter)
ε_0 = dielectric constant of vacuum or air (= $8.85 * 10{-}12$ farad/meter)
ε_r = relative dielectric constant

According to the following equation where $\mathbf{v}_m$ is GPR waves velocity, c is speed of light and $\boldsymbol{\varepsilon}_r$ is dielectric constant of the medium material.

$$\mathbf{v}_m = \frac{c}{\sqrt{\varepsilon_r}}$$

It is clear from the equation that if value of dielectric constant is higher, lower will be the velocity of GPR signals and if dielectric constant value is lower the velocity of GPR waves will be higher. It means a material having low dielectric constant will allow the GPR waves to move faster and vice versa. Velocity of GPR waves is inversely proportional to the dielectric constant of the material. In actual GPR instrument measures the time taken by the EM wave transmitted from the antenna to material and reflect to radargram (Which Velocity Should I Use for My GPR Investigations and Why? n.d.). For that purpose, velocity of the GPR waves is critically important to find the actual distance from antenna to the encountered object by EM waves as shown in *Figure 5* .

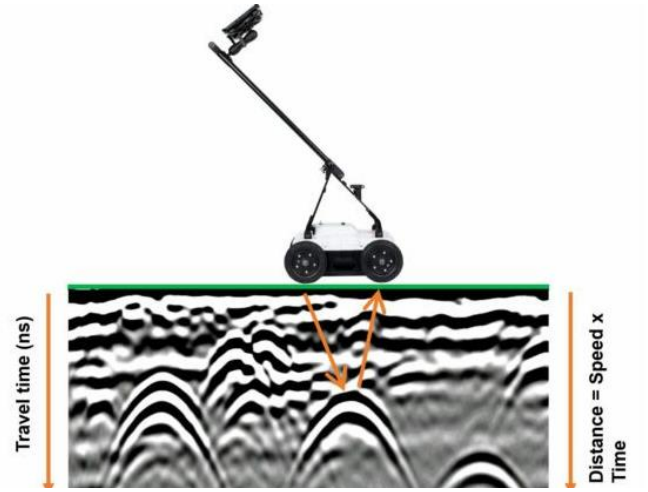

Figure 5- Transmition and reflection of EM waves (*What Is a Trace? - Guideline Geo*, n.d.)

According to (Evans et al., 2007) passage of the EM waves depends on the host material properties like material type, condition and moisture content and these properties cause an effect on the dielectric constant of the material which decides the travel time and speed of EM waves through the material. (Alsharahi et al., 2016) says that information about the electrical properties of the beneath surface to GPR antenna are very important to predict the behaviour of the antenna and in this scenario dielectric constant of the material is very important to find the velocity and depth of the detected objects.

Above mentioned reasons state the importance of the dielectric constant or relative dielectric permittivity (RDP) in GPR technique to find the velocity of

EM wave pulse, return time of signals to antenna and depth of the detected objects in the host material and it varies from material to material.

2.1.3 Concrete scanner – GPR system

GPR work is based on the travel time of the electromagnetic signals in the material and measurement of the amplitude of the reflects electromagnetic energy waves(Parrilla, n.d.). According to the GPR working principle, hardware of the GPR includes a wave form generator, a single transducer comprised of transmitter and receiver antennas which also referred as Rx and Tx, a processing unit for signal processing and a data storage system (Yazdani et al., 2018). According to (*What Is GPR: A Brief Description by GSSI*, n.d.) GPR includes three components as shown in *Figure 6*.

- Control Unit
- Antenna
- Power Supply

Figure 6- GPR Instrumentation (*What Is GPR: A Brief Description by GSSI*, n.d.)

- Control Unit

Control unit of GPR contains electronics and electrical system which trigger the pulse of EM waves, it means control unit performs EM wave or pulse generation and can be called as wave from generator. Generated EM wave pulse by the controller sent to the material by the antenna. Control unit is built in computer having storage system to store GPR field data for afterwork analysis. After work analysis of GPR data is done by the computer-based software relevant to variety of the GPR types. Control unit types are different in the different GPR instruments. (Lachowicz & Rucka, 2015) used GPR Alladin Structures Kit system comprised of control unit, antenna, and portable com puter and batteries.

Depending on the different type of GPR instruments, GPR apparatus varies accordingly like concrete scanner used in this thesis work includes all three main components in single instrument called PS 1000 X-SCAN CONCRETE SCANNER.

- Antenna

Common radar antennas are divided into two types, Ground couple antenna and air launched antenna. (Eide et al., 2014) worked on the design of ground coupled antenna to achieve the frequency range from 100MHz -3GHz using monopoles to obtain the optimized results operating directly on to the ground surface. To obtain the shallow image of the concrete rebars it is highly important to keep small distance between transmitter and receiver (Rx and Tx). Hence monopoles are arranged in specific arrangement in a way to keep the feed points as close as possible to simulate zero-offset antenna structure. Mostly ground coupled antenna system is preferred to air launched antenna for greater depth penetration due to low frequency range, that's why it provides the low resolution of the images. It varies from instrument to instrument as in PS 1000X Concrete scanner uses the ground coupled antenna with 2GHz maximum frequency with penetration depth of 300mm. Three antennas are placed at the bottom of the instrument as shown in *Figure 7*

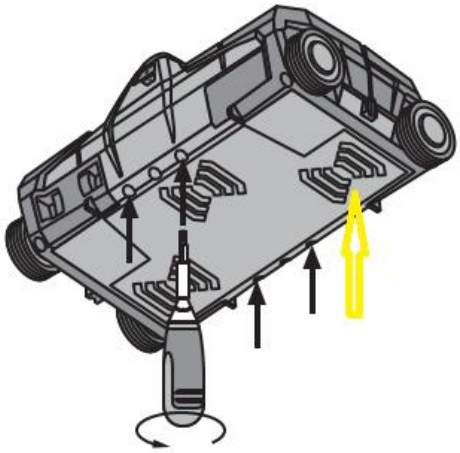

Figure 7- GPR Antennas

Air launched antenna is named air launched as it remains in the air above the ground 30 to 50cm. Air launched antenna operates higher frequency range and does fast scanning than ground coupled antenna. Structure of typical air launched GPR unit includes transmitter, a receiver, storage system and control unit with display and power supply(Khamzin et al., 2017). Air launched antennas with high frequency range (0-2000MHz) are typically used for the condition assessment of concrete structures and to find the layer thickness of pavements. *Figure 8* shows the structure of air launched antenna GPR system.

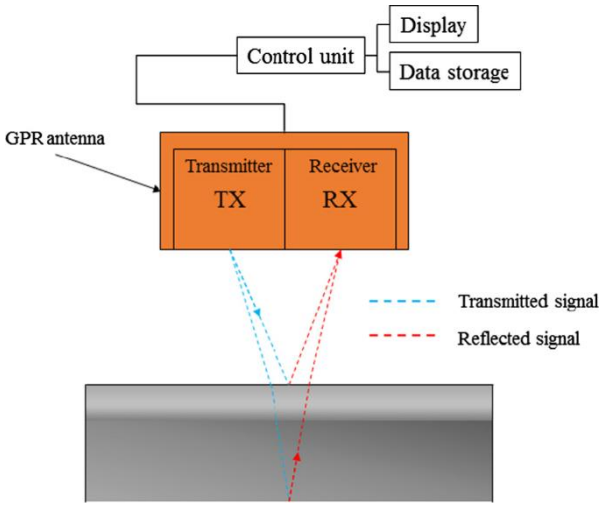

Figure 8- Air Launched Antenna (Khamzin et al., 2017)

According to GPR antenna positioning with respect to the scanning surface GPR data collection is divided into ground coupled and air launched antenna surveys. When antenna is placed at the testing surface, the EM waves are pulled by the concrete/ground then antenna becomes ground coupled system. This data collection system is preferred to air launched system as it avoids the gap between the antenna and concrete surface. when antenna is kept at a certain distance from the concrete/ground radiated EM energy makes a big cone and this system is called air launched antenna GPR system. Data acquisition methods (A, B, C and D scanning) – principles with images and illustrations (Neupane, 2020).
GPR survey provides the radar scans not the actual pictures of the subsurface area. There are three different ways of the presentation of GPR scans as following:

A- Scan

The plot between the intensity of EM wave reflections in Y-axis and time travel on the X-axis due to result of point measurement is called A -Scan of the GPR image. In other words, A- Scan is the raw scan obtained by the antenna is function of time and EM wave signal strength or amplitude of the reflected EM signal. In case of known velocity of the EM propagation wave, time travel in the X-axis can be transferred to the depth scale too. Basically A- Scan is one dimensional trace of the GPR survey. Vertical deflected lines in *Figure 9Figure 9* are representing A-Scan.

B- Scan

Most common used images in the GPR survey are 2D scans or vertical profiles and called radargrams. In B-Scan depth is presented on the Y-axis and survey distance is shown on the X-axis (Hammarström, n.d.) . Result of radargram is equivalent to the slice of perpendicular through the plane in trace

direction and in B-Scan representation of intensities is in two-dimensional way as pixels in the signed colours or grey scale (Konrad Topczewski et al., 2007). As shown in *Figure 9* antenna, transmitter and receiver are moved in the direction of survey line and in case of recording of whole trace, a plot of A scan on the surface is called B-Scan or radargram

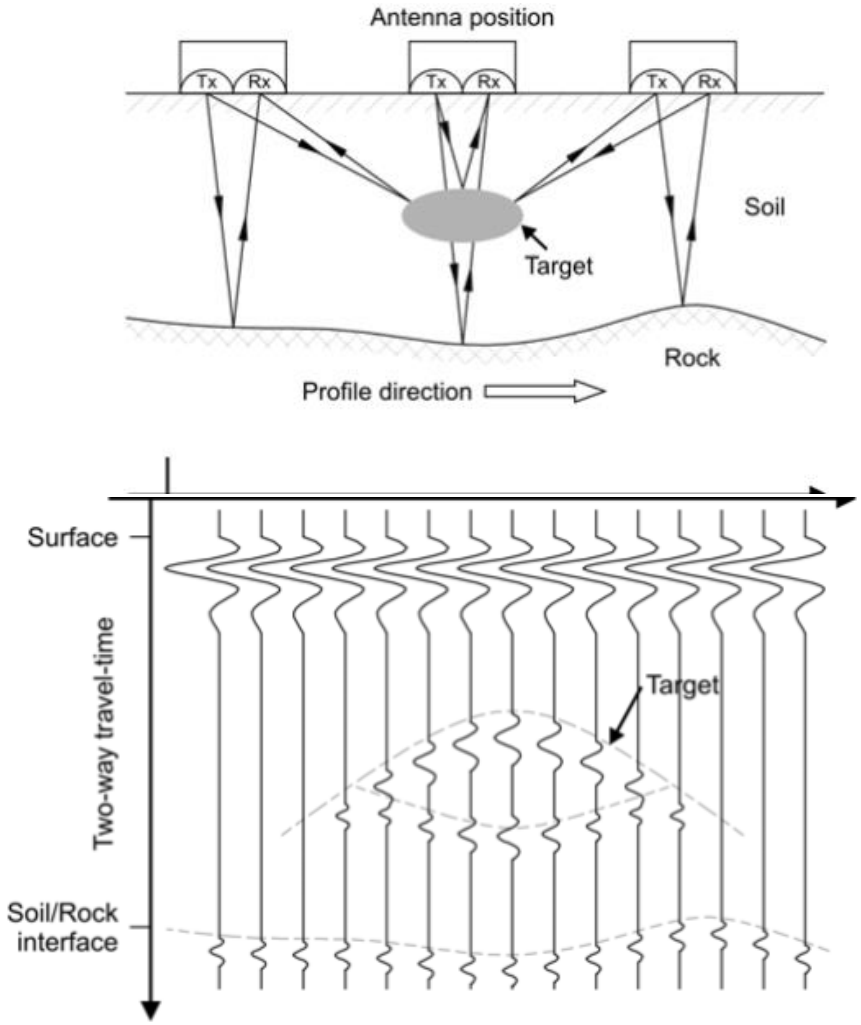

Figure 9- A Scan & B scan by GPR system

C- Scan

3D map of the subsurface area by collecting the individual grid of the B-Scan or radargram is called C-Scan. This technique provides the 3D volume of the radar data by obtaining a dense subset of the parallel 2D profiles from the B-scan, as shown in *Figure 10*.

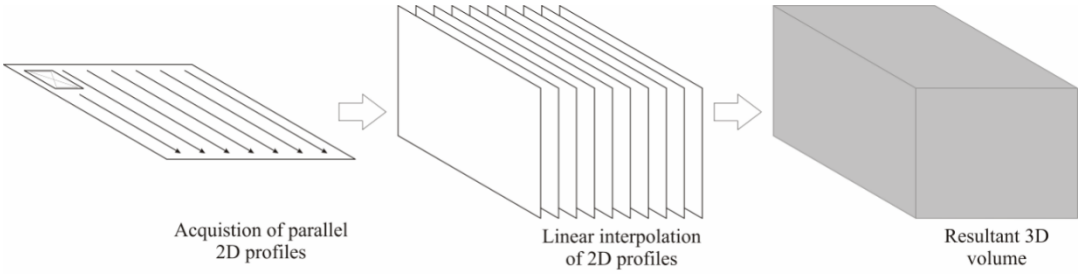

Figure 10- 3D Scan or C scan

2.1.4 GPR data processing

GPR data is obtained in raw form from the site location in the shape of scans, images, or recordings. According to GPR, working principle, l EM waves are sent to ground or concrete and reflected echoes in the form of signal traces with the movement along survey line, also called A- Scan. If this data is collected in the form of a 2D scan is called B-Scan and with the movement of antennas in tow dimensional three-dimensional images (C-Scans) are achieved (Szymczyk & Szymczyk, 2013). Obtained images from this type of data is challenging to understand due to scattering and diffractions and processing of these images (data) is necessary to obtained accurate results. Obtained raw data or GPR scans are not cleaned and contaminated by different anomalies in the concrete or soil influences the scans to be cleaned to make the details visible and transparent.
GPR data processing consists of three major tasks:

1. Data processing and interpretation
2. Pre-processing phase, signal, and image processing techniques
3. Signal Processing

Table 1- Basic Steps of GPR Data Processing adopted from (Szymczyk & Szymczyk, 2013)

Editing	Removal and correction of bad/poor data and sorting of data files
Rubber- Banding	Correction of data to ensure spatially uniform increments
Dewow	Correction of low-frequency and DC bias data
Time Zero Correction	Correction of start time to match with surface position
Filtering	1D & 2D filtering to improve signal to noise ratio and visual quality
Deconvolution	Contraction of signal wavelets to" spikes" to enhance reflection event
Velocity Analysis	Determining GPR wave velocities
Elevation Correction	Correcting for the effect of topography
Migration	Corrections for the effect of survey geometry and spatial distribution
Depth Conversion	Conversion of two-way travel times into depths

Display Gains	Selection of appropriate gains for data display and interpretation
Image Analysis	Using pattern or feature recognition tools
Attribute Analysis	Attributing signal parameters or functions to identifiable features
Modelling Analysis	Simulation of GPR responses

Focus for data processing is signal processing as antenna (receiver) receives the reflected EM waves in the form of signals.

GPR signal Processing:

Digital signal processing is normally required to filter the raw data including removing of unwanted noise, signal strength balancing and correction of variations in topographic elevations (Yelf & Yelf, n.d.). In actual received signal is the first echo of air-ground interface and later appearance of reflection on target and background noise due to subsurface reflections which is also called clutter in the subsurface. Removing of clutter is the priority in the data processing. Signal processing includes following tasks:

- **Time Zero Correction:**

Time delay and reduction in the frequency of the signal happens due to coupling effect. Coupling effect occurs between the radar signal and material of the ground or concrete and being sensitive to temperature, moisture, and distance of antenna from the ground surface affects the shape of the signal (*Post Processing GPR Data | United Scanning Services*, n.d.). Basically, time zero correction is adjusting the vertical position of the subsurface reflection at time zero position (Yelf & Yelf, n.d.). The time when signal/wave leaves the antenna and enters in the subsurface is called time zero and time zero correction is very important to adjust all the traces to the common time zero position (Szymczyk & Szymczyk, 2013). Time zero correction is performed toa assign the top of the scan to the exact ground level this step is very important using air launched system for the survey (Neupane, 2020). In road surveys fixation of time- zero point is strictly necessary to compare the reflection time and depth of inhomogeneities at different locations in the pavement and it cannot be ensured due to different factors like different temperature of the air during data collection, length difference of connecting cables, difference of antenna heights because of vertical acceleration acting on instrumented vehicle. Due to above factors variation in position of reflection coming from air pavement interface. To avoid all the above-mentioned problems common time- zero position correction of the data is highly important(Benedetto et al., n.d.). Following *Figure 11* is showing the difference of data interpretation before and after time-zero correction.

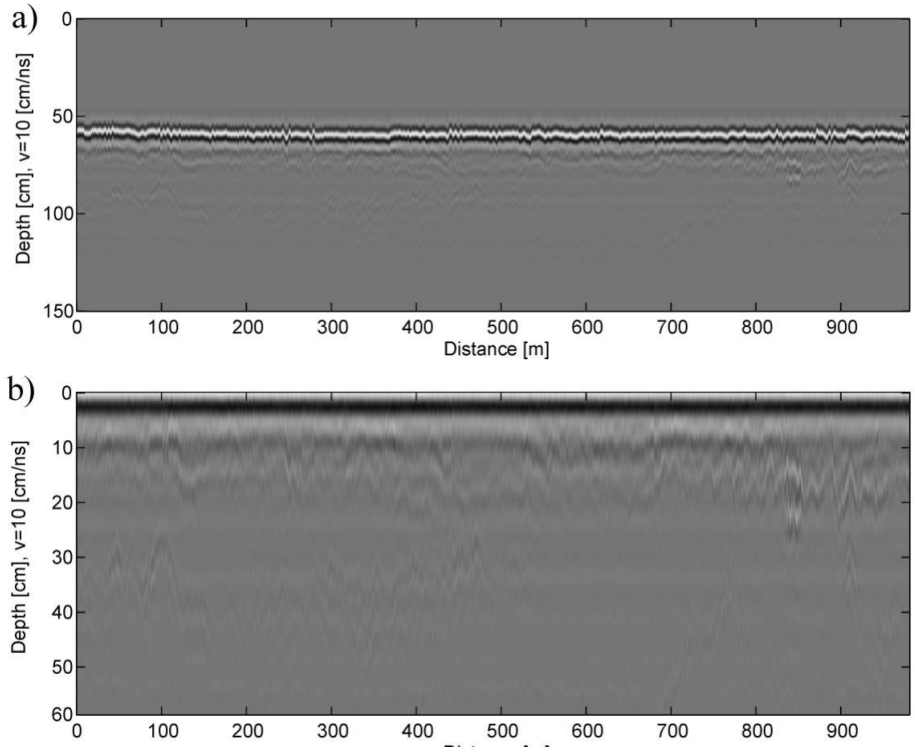

Figure 11- Time Zero Correction in GPR data processing

Removal of Background:

Using horizontal high pass filter to have a difference between real reflected signal from the target and clutter or noise in the background. Except real signal background noise is removed from the GPR scans or images (*Post Processing GPR Data | United Scanning Services*, n.d.). It also includes the radargram size reduction by discarding the late time arrival reflected signals. It is also named as band- pass filtering to remove unwanted high or low frequency. There are different types of filtering used for background removal like Band -pass filtering, average filtering, deconvolution filtering (to remove unwanted echoes and ringing) (Yelf & Yelf, n.d.).

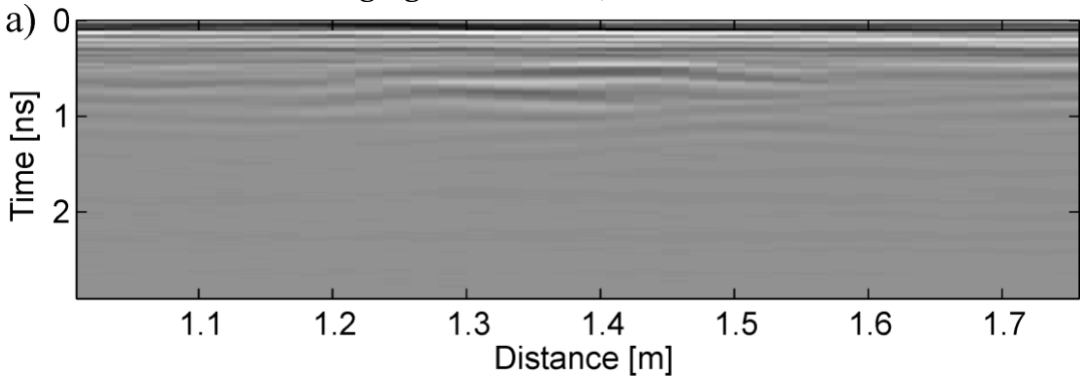

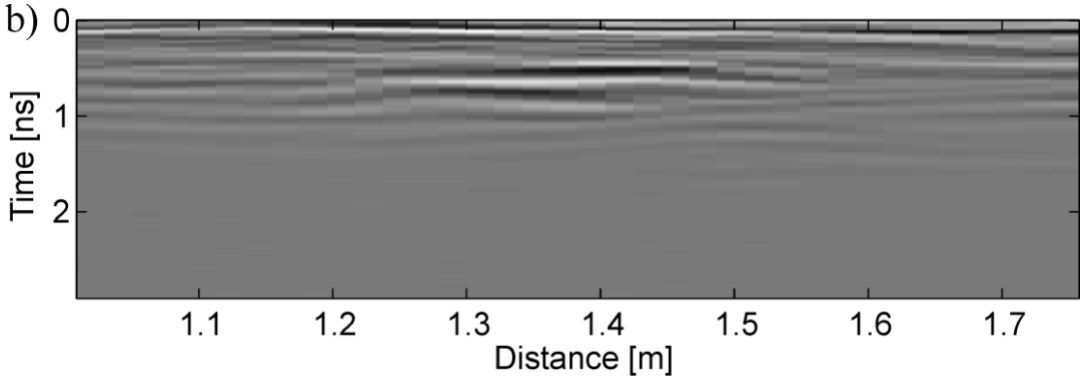

Figure 12- Background Removal in GPR data processing

Gain Correction:

According to (Yelf & Yelf, n.d.) to increase the signal magnitude or amplifying of signal is called gain and gain correction helps to make obvious areas of interest in the scan. By applying multiplier effect to the interested regions of the scan in terms of time and intensity of the reflected signal to make clearer and recognizable against the background of the scan. predefined colour schemes are also applied to the data to have different indications of objects and background.

Migration:

according to working principle of the GPR, it produces the cone and reflected signals from reflections are basis of the image produced. At the edges of the cone signals cover long journey than the signals reflected from target closer to the centre of the cone. This phenomenon is base of the hyperbola curve in the GPR scan. To resolve hyperbola curve in the scan, application of complex mathematical algorithms to the scanning data to obtain precise representation of target is called migration technique in GPR image processing (*Post Processing GPR Data | United Scanning Services*, n.d.).

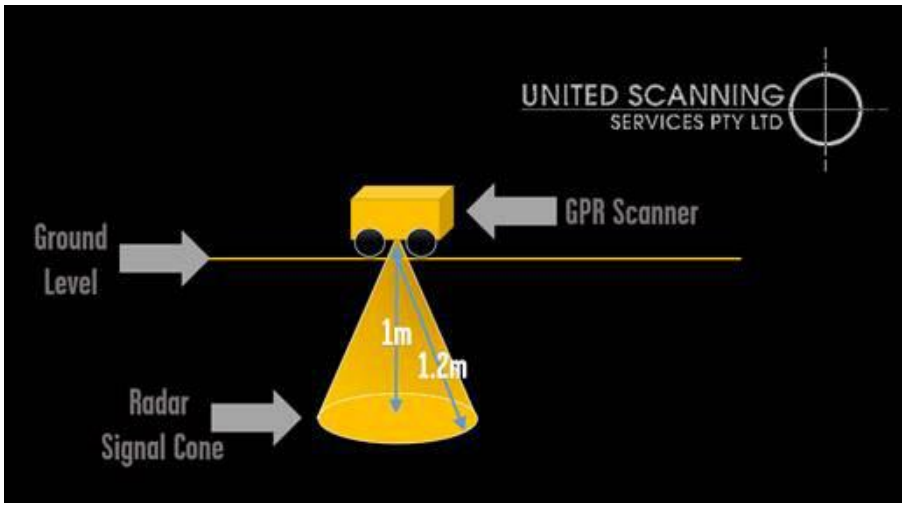

Figure 13-GPR produces a signal cone which results in targets appearing as a hyperbola (*Post Processing GPR Data | United Scanning Services*, n.d.)

3D Rendering:

3D rendering provides the detailed view of GPR scan after processing of GPR data in the forms of A-scan, B-Scan. Conversion of B-Scan in 3D visualization is called 3D rendering of the GPR scans.

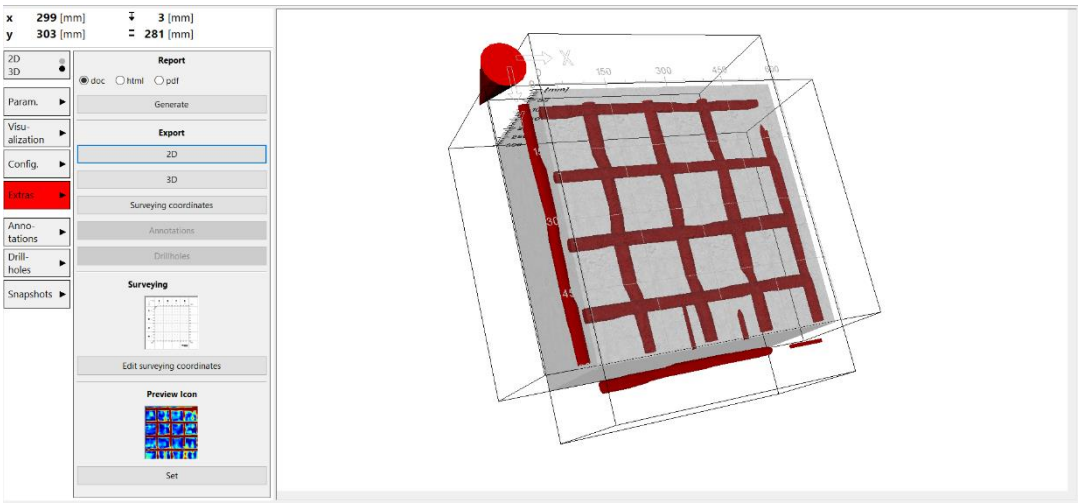

Figure 14- 3D Rendring (Profis Detection Software)

2.1.5 Hyperbola fitting

The procedure used for estimating of the average velocity of the GPR signals reflected from metal objects or different anomalies in subsurface is called hyperbola fitting. As GPR emits the signals in shape of cone in the subsurface, signals at the edges take time to reach the target than the signals near the centre of the cone. If target is not directly in the centre of the cone, returning signals take time and position of target appears deeper in the scan and in case of presence of target in the centre of the cone target appears at lower depth due to less time in returning of signals. Since passing of scanner over targeted

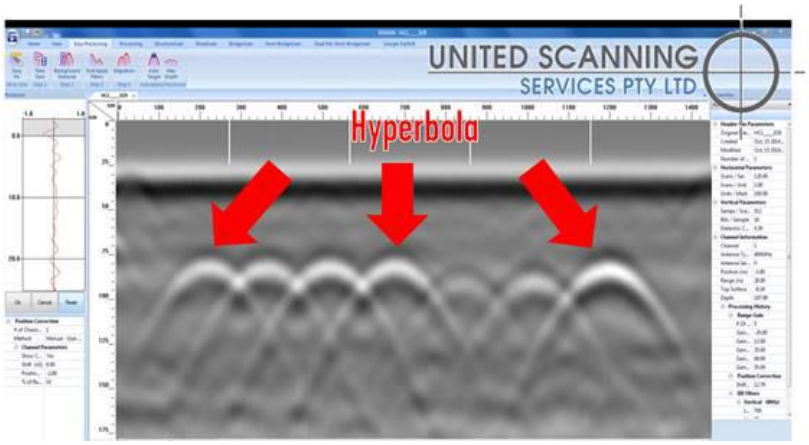

Figure 15- The appearance of hyperbola in a scan(*Post Processing GPR Data | United Scanning Services*, n.d.)

object makes the hyperbolic shape of reflected signals on the radargram(*Post Processing GPR Data | United Scanning Services*, n.d.).

Essential need of hyperbola fitting is to approximate a possible depth scale to find the depth of reinforcement in the subsurface from hyperbolic shapes(*MALÅ Easy Locator Pro HDR Series User Manual*, n.d.). GPR transmitting antenna radiates the EM waves in the conical form and angle range of cone apex is 60 to 90 degrees and hyperbolic shapes are obtained on the radargram when antenna crosses the metallic objects (steel reinforcement, pipes) located perpendicular to the antenna path. It means that antenna will detect the target when it is directly above it or in the centre of conical bans of EM wave but also from after and before the target location (Morris, 2004). (Dou et al., 2017) applied a machine learnt model in identification of hyperbolic signatures to fit the hyperbolic curves to each other to obtain the relevant and related parameters those can be used to estimate the location and size of the targeted object and signal propagation in the medium of the material.

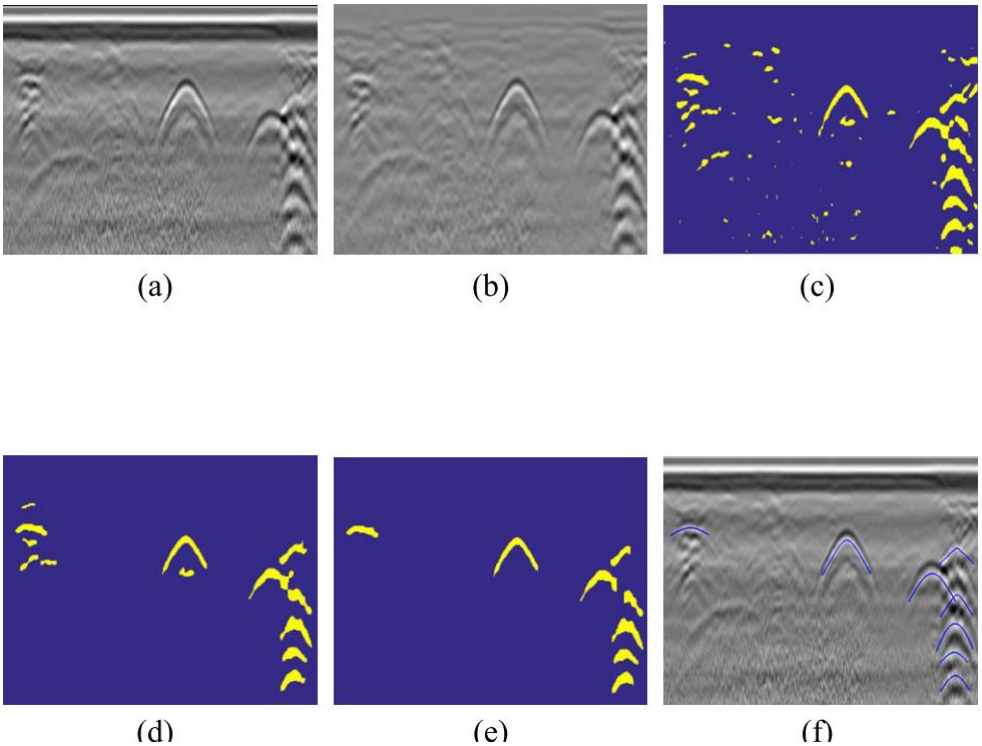

Figure 16- (a) Input image. (b) Image after preprocessing. (c) Regions of interest after thresholding. (d) Clusters after applying the C3 algorithm. (e) Identified hyperbolic signatures by applying the machine learning algorithm. (f) Output image from the system with fitted hyperbolae. Intersecting—with crossing tails, connected without crossing tails. Distorted—asymmetric or incomplete (best viewed in color).(Dou et al., 2017)

2.2 Defects in reinforced concrete structures

Reinforced concrete structures undergo with mechanical usage, environmental effects, and weather attacks. These three phenomenon cause defects in the reinforced concrete structures. In concrete problems defects are crucial important to get notified and eradicated for long life and durability of the reinforced concrete structures. In general, different mechanism are play their role in problems of reinforced concrete structure and they are classified as following:

Defects: Causes of defects in RC structures are design, material, and construction

Damage: concrete structures are vulnerable to overload, fire impact and chemical spill damages

Deterioration: deterioration of reinforced concrete structures is metal corrosion, erosion, freeze & thaw action, sulphate attacks, and time dependent chemical changes (Al-Neshawy, Ojala, et al., n.d.).

Defects are the vital cause of failure of the concrete structures and need to be investigated and inspected for maintenance and repair of the structures. For frequent condition assessment of concrete structures non-destructive and non-invasive techniques are always preferred. Visual defects can be easily seen and assessed but sub surface defects are vital important to be detected and repaired. For subsurface detection of the defects and problems most common instrument used is GPR with different frequency ranges. Since detection of subsurface defects is highly preferred as bridges mostly fail due to occurrence and propagation of subsurface defects. Subsurface defects include internal cracks, voids, and subsurface delamination. Subsurface or internal cracks in reinforcement concrete structures occur due to corrosion of reinforcement. Oxide layer formation on the rebar surface creates tensile stresses in surrounding concrete resulting cracks in around the rebar and cracks propagates with the increase of corrosion (Aggelis et al., 2010).

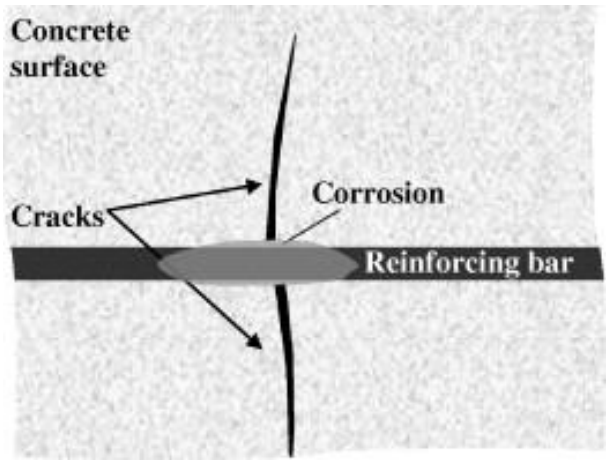

Figure 17- Development of subsurface cracks by corrosion of rebar.(Aggelis et al., 2010)

Another defect is subsurface delamination which develops inside the concrete surface mainly due to corrosion of reinforcement, freeze and thaw action and mechanical damages to the concrete structures as traffic loading and operations on the bridge decks. Delamination caused by development of internal cracks can be seen from naked eye but difficult to measure the defected area in the subsurface of the concrete. For detection purpose NDTs are used but still difficult to recognize the defect (Tran et al., 2018).

Creation of subsurface voids or internal voids is majorly poor consolidation of the fresh concrete, during pouring of fresh concrete air penetrates the material and due to poor use of vibration for consolidation air bubbles entrapped and creates the air pockets or subsurface voids in the concrete surface. Early age detection and checking of voids is almost impossible due to small size and tightly packed. Voids damage the integrity of the reinforced concrete structures and leads to the failure of the infrastructure. Since timely inspection and detection of these voids and evaluation of the subsurface defects is primarily important for health monitoring of RC structures(Yang et al., 2020).

2.2.1 Construction defects

Construction defects directly affecting the performance and durability of the structure can be the result of defective construction and improper design of the structure. Construction defect can be defined as the problem or deficiency in the design, construction quality, use of bad quality material and poor workmanship during execution of the project. Premature failure of a structural element/ component causing damage to human/structure is called construction defect (Jaydeep et al., n.d.). In general construction defects occur during design and execution of the project. Two main reasons of the construction defects are improper design and poor workmanship. Design errors occur due to reduction of column and beam sizes to save the cost and in this way, structure face the collapse by not fulfilling the main purpose. Faulty construction is main reason of the structural collapse and building defects (Ahzahar et al., 2011). Lack of supervision at construction site causes rework and affect the construction quality of the project.

If design of a structure is not according to the design codes and details and execution of the project doesn't happen according to the proper construction rule and skilled labour, chances of construction defects are higher in this case. Some construction defects are visible and can be inspected with naked eye like spalling and peeling off plastering from the walls. subsurface defects due to defective construction like honeycombing, internal voids, misalignment during installation of formwork, premature removal of formwork, misalignment and detailing errors in the rebar schedule are unable to detect and

inspect in the concrete structure with naked eye. Since non-destructive techniques are used for this purpose including Schmidt hammer and GPR. Major contribution to poor workmanships is unexperienced labour lacking technical knowledge, resulting the poor quality of construction work. Construction defect like segregation happens due to poor workmanship and results creation of voids in the concrete. These effects make concrete vulnerable to degradation and lack of performance. Insufficient concrete coating causes corrosion of reinforcement. Corrosion and segregation cause bearing capacity of the reinforced concrete structures (Obiora et al., 2022).

Table 2- Types of construction and common building defects and their symptoms (Jaydeep et al., n.d.)

Defects	Symptoms	Possible Cause
Concrete spalling and loose plaster in ceiling	Exposure of reinforcement due to falling of cement plaster, patterned cracking, surface with water satins	as a result of aging in old buildings, reinforcement defects due to persistent water leakage, use of salty wate in concrete preparation
water seepage from wall, roof and ceiling	Fungus growth, water stains, peeling off paint and paper,	Due to external water seepage in the result of minor cracks on the wall, honeycomb concrete
Structural cracks in walls	Continuous cracks across width of the wall, diagonal cracks, penetrating cracks through bricks and finished surface, contaminated cracks with rust	Unwanted ground settlement, sewer overloading, weakness of structure due to corrosion and deterioration of materials, accidental damage and poor design/ construction
Structural cracks in columns and beams	Penetration of cracks through finishes down to the bricks and reinforcement	Unwanted ground settlement, sewer overloading, weakness of structure due to corrosion and deterioration of materials, accidental damage, and poor design/ construction
Non structural cracks	Multidirectional cracks, shrinkage cracks	Hailine cracks due to cosmetic shrinkage cracks in plaster affecting aesthetics of the structure.
Defective external wall finishes	Debonding of finishes, from wall structure in the	Aging, structural movements, poor quality construction, execution by

	result of hammer tapping. Loosening of parts,	non-skilled labour, defective or missing expansion joints.

Honey Combing

According to (Subakaran & Herath, n.d.) honeycombs and air voids are trapped in concrete surface due to segregation effect and improper consolidation of concrete. Formation of honeycombs is on the concrete surface gets visible after removing the formwork. Use of larger size aggregates, stiff concrete and improper vibration are main causes of honeycombing in concrete. Occurrence of honeycomb and rock pockets in the reinforced concrete structures happen due to mortar paste failure to occupy the spaces around coarse aggregates. Honeycombs and rock pockets are called local and internal defects. There are several reasons causing honeycombs and rock pockets like poor quality control in concrete mixing, chances of segregation during transportation of concrete mix, pouring of fresh concrete, under and over vibration/compaction of concrete, insufficient spacing in the rebars for proper mortar paste flow and low cement content(Sezer Atamturktur et al., n.d.). This spectacular defect causes strength reduction of the concrete structure and makes it highly vulnerable to degradation and deterioration depending on the size of the defect. There is vital role of proper consolidation in hydration process of concrete and in strength development and durability of the concrete structures. According to (McCabe et al., 2021a) honeycombs and rock pockets are construction defects and responsible for premature deterioration of concrete and their effects are more lethal than load and thermal effects. Honeycombs are basically internal voids with different size and shapes and mostly appear on the concrete surface with improper finishing and sometimes these occur in the subsurface of the concrete. Honeycombs also cause the debonding of rebars and mortar paste due to insufficient rebar spacing. During placement or concrete pouring process improper consolidation between cement mortar and coarse aggregates causes creation of large voids in the concrete surface. Rock pockets fall off form their place with time and debonding factor. Honeycombs and rock pockets severely affect the concrete strength and durability due to reinforcement exposure to environment in case of fall off from their places due to debonding.

Foreign objects – images

Foreign or embedded objects in concrete structures are simulated defects installed during construction of concrete structures for testing and investigation purposes. On the other hand, prestressed conduits, electrical wiring pipes are also considered as foreign or embedded objects in the concrete structures. Figure () shows the simulated defects installed in the mock up wall for testing purpose. Figure () shows the reinforcement details and there is prestressed conduit which also refers the foreign objects in the concrete structures.

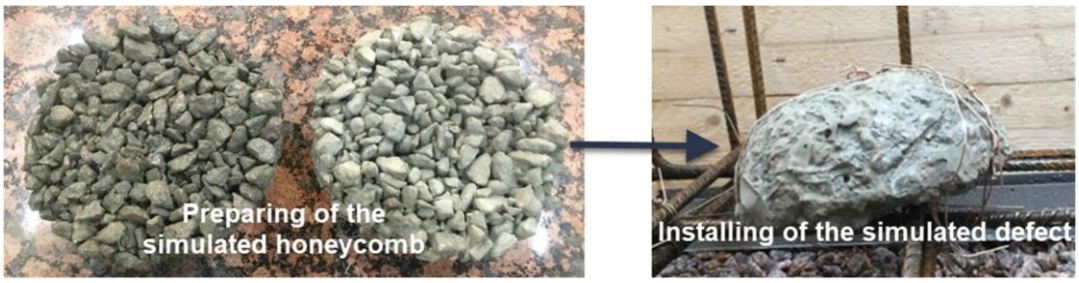

Figure 18- Use of different density simulated honeycombing in the base slab of the mock-up wall (Al-Neshawy, Ferreira, et al., n.d.)

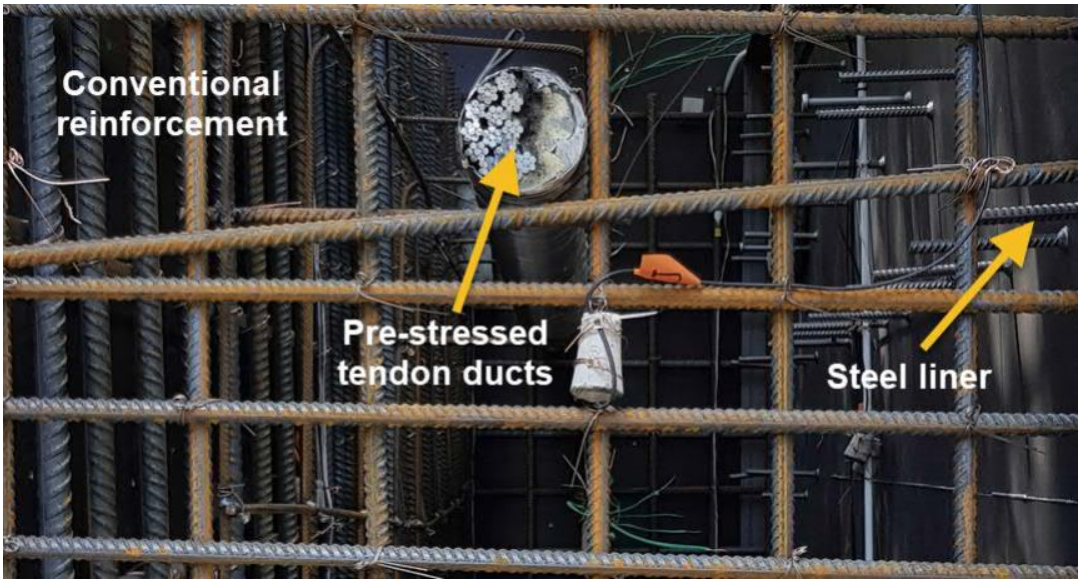

Figure 19- Mock Up Wall Reinforcement (Al-Neshawy, Ferreira, et al., n.d.)

Cold joints

According to (Yoo & Kwon, 2016) occurrence of cold joints in concrete structures is due to delayed new concrete placing and poor condition of the old concrete surface. Penetration/ingress of chloride in cold joints is much rapid than in the sound concrete and it is also vulnerable to be affected by the loading conditions. Cold joint is a type of construction defect occur in the result of concrete pouring in intervals, if it gets delayed chances of cold joint formation increases. That's why concrete pouring should be done/completed in one go without interruption to prevent the creation of cold joints. (Bekem Kara, 2021) says that during execution at construction site concrete placement must be made as continuous as possible. In usual practice concrete pouring happens batch wise depending on the construction site, lack of formwork/ moulds, difficulty to produce bulk (production of total volume at once) volume of concrete and transportation problems hindrances the pouring and placement of concrete at once. Limited manpower and procurement are also causes of batchwise pouring of concrete. Keeping in view above mentioned reasons concrete is poured batchwise/stepwise. Formation of cold joint happens when earlier placed concrete hardens before the pouring of next batch

of concrete (Hashemi et al., 2018). Hot weather and windy conditions during concrete placement also lead the formation of the cold joint in concrete. Performance and durability of concrete structures are directly affected by the presence of cold joints.

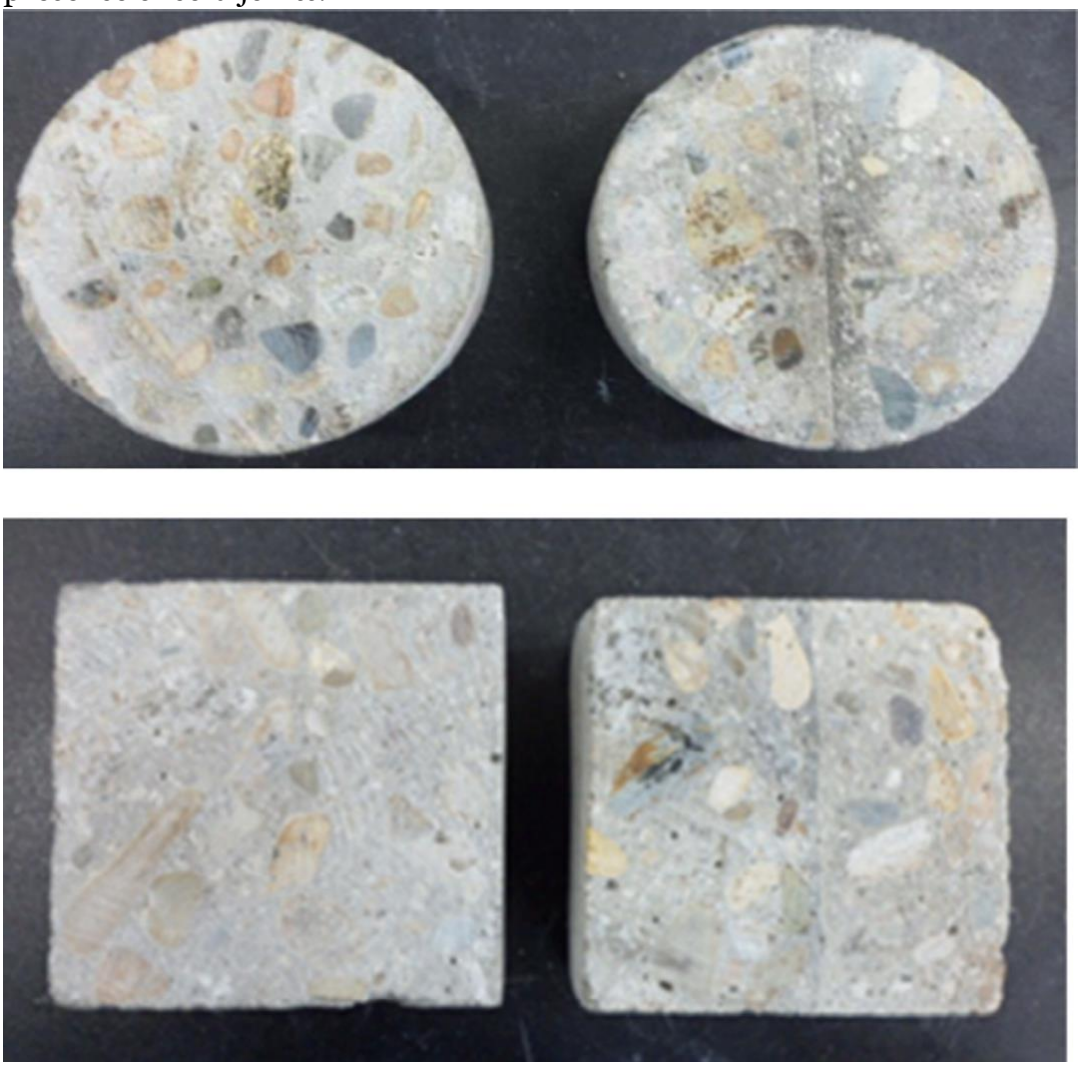

Figure 20-Compressive and tensile strength samples with cold joint -(Yoo & Kwon, 2016)

2.2.2 Ageing and environmental defects

Reinforced concrete structures undergo degradation and deterioration phases in their whole service life. Degradation is the major cause of reduction of service life of the structures resulting in social, environmental, and economical damage. Most of the degradation processes includes climate variables and external environmental effects like temperature, relative humidity, precipitation, wind waves and tides (Medeiros-Junior, 2018). Exposure of concrete structures to environmental factors like climatic attack, chemical attacks, abrasion, wear & tear, freezing and thawing action and sulphate attack in marine environment make it highly vulnerable to degradation and

reduction in its service life (Chemrouk, 2015). The major cause of deterioration and degradation of concrete structures from environmental factors is freeze and thaw action. During freezing and thawing action internal and external damages do occur. External damages include the scaling and spalling (erosion) of thin outer layer and aggregates of concrete due to weathering attacks (de-icing salts) and outer damages do not affect the mechanical properties of the concrete structure, but it leads the chloride penetration and leads to corrosion of reinforcement. Internal damages include microcracks in the cement paste (*Influence of Freezing and Thawing*, n.d.).

Steel reinforcement defects

Performance of reinforcement concrete structures is adversely affected by the degradation of reinforcement in concrete structures. The prominent reinforcement defect is corrosion of steel rebars with passage of time and chloride ingress in the reinforcement concrete structures. Corrosion is rust formation on the steel rebars which increases the volume of the bar and cause tensile stresses around the rebar surrounding. As concrete is weak in tension, so cracks occur which leads the concrete to spalling and cracking (Al-Neshawy et al., 2016). Corrosion of reinforcement is a complex electrochemical process which depends on the permeability, electric potential, and concrete resistance to electrical conductivity. Occurrence of corrosion happens in the presence of oxygen and water resulting formation of iron oxide which is called rust (Bonić et al., 2015). Due to corrosion effective area of steel rebar decreases which causes strength reduction and decrease the service life of the structure.

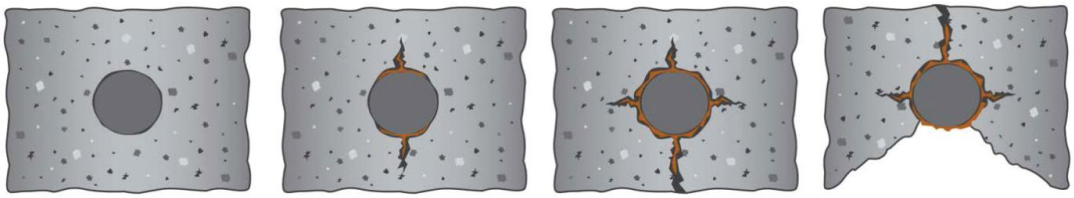

Figure 21-Development of corrosion of a reinforcement bar in concrete.(Bonić et al., 2015)

Major causes of reinforcement corrosion are carbonation, acidic gases penetration, chloride ingress, concrete quality, w/c ratio of the concrete mix, cement content, impurities in the concrete ingredients, appearance and presence of surface cracks and other environmental effects like moisture, humidity, bacterial attack, and temperature affect the corrosion process of steel reinforcement (Ahmad, 2003).

Deterioration phases for concrete structures

Deterioration of reinforced concrete structures is divided in two types depending on the nature of the deterioration. Physically induced deterioration and chemically induced corrosion. Physically induced corrosion is also called

external deterioration which includes mechanical abrasion, erosion, cavitation, and freeze-thaw action. Chemically induced corrosion includes carbonation, chloride ingress, corrosion, acid attacks, alkalis effect on specific aggregates in the concrete mix design, and sulphate attacks (Penttala, n.d.). Occurrence of deterioration and degradation of concrete structures mainly by physical processes or chemical reactions. According to plethora of reports and research work done till now, reinforced concrete structure is highly vulnerable to the corrosion of reinforcement. Preventive measure for corrosion of steel rebars is only provision of sufficient concrete cover and protection from the alkaline surroundings (Malioka, n.d.).

According to (Al-Neshawy et al., 2016) deterioration of concrete structures estimation is conducted in three different phases:

1. 1st phase of deterioration starts after the construction and before start of reinforcement corrosion.
2. 2nd phase is the period between corrosion initiation and cracks occurrence. Reinforcement corrosion happens in two phases, initiation phase and propagation phase. In initiation phase structure doesn't feel the weakening in strength but passive layer around the rebars starts destabilizing under the effect of presence of chlorides and carbon dioxide. Initiation phase lasts with the start of corrosion of the outer layer of reinforcement when chlorides and carbon dioxide concentration exceed from a critical value. In propagation phase corrosion prevails and effective cross-sectional area of the rebar decreases, rust formation happens on the rebar surface, and rust volume increases resulting the expansive (Tensile) stresses in surrounding concrete resulting the cracks which leads the structure to failure eventually (Malioka, n.d.).

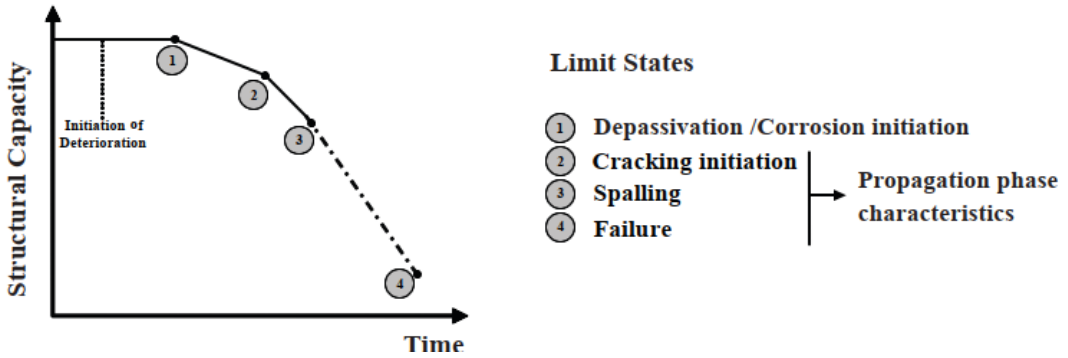

Figure 22- Corrosion phases of concrete structures (Malioka, n.d.)

3. 3rd phase is from crack formation in the structure to the failure of the concrete structures.

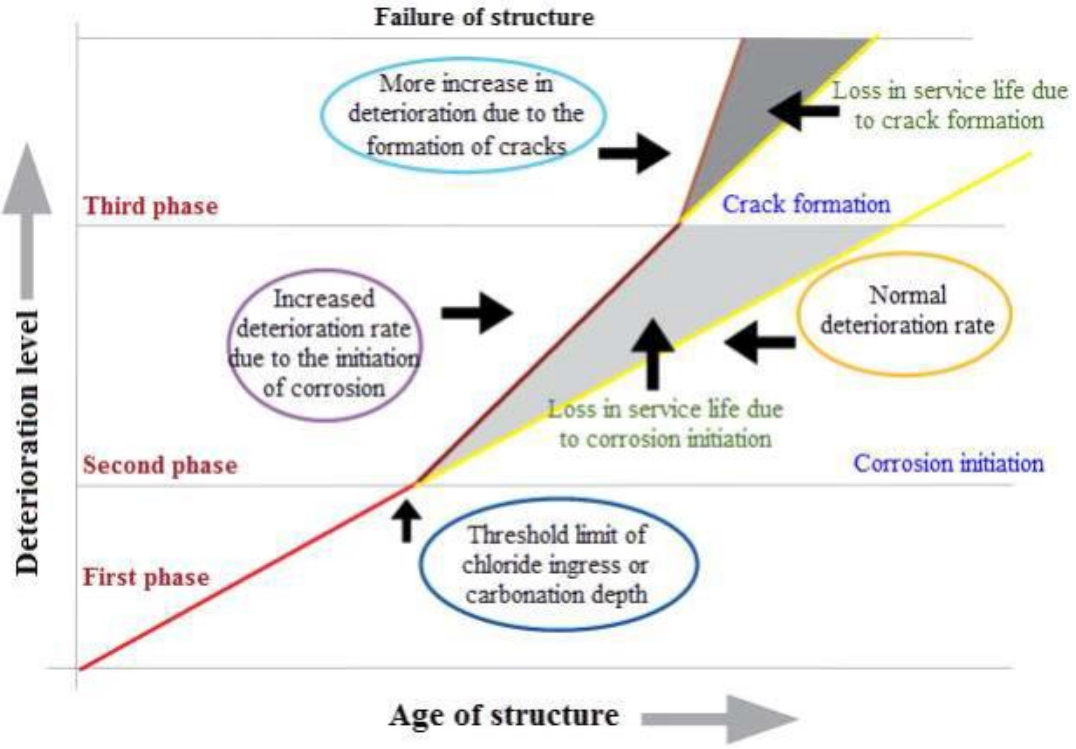

Figure 23- Main events related to the service life of concrete structures (Al-Neshawy et al., 2016)

Figure 23 represents the events related to the service life of the concrete structures and three different phases of the deterioration. According to the deterioration phases involved (Al-Neshawy et al., 2016) recommended the selection of non-destructive techniques and their division according to the three different deterioration phases.

In 1st phase of deterioration selection of NDT methods is primarily based on the monitoring of actual conditions like execution details, homogeneity and quality of construction which affects the design life of structure. Detected construction defects can be eradicated to save the expensive repairing costs at the final stage. Detection of honeycombing, carbonation depth measurements, estimation of chloride content, concrete cover thickness and measurements related to quality of concrete are detailed examples of NDT testing in 1st phase (Al-Neshawy et al., 2016).

In 2nd phase during operation structures are monitored including visual inspection of visible defects on the surface and subsurface defects (internal voids, cavities and internal cracks) are needed to be inspected and detected using NDT methods (Hammarström, n.d.). During initiation phase NDT methods are intended to for concrete cover examination which is highly vulnerable to deterioration from mechanical and chemical attacks.

In 3rd phase use of NDT methods is intended to assess the cracking, delamination, corrosion of reinforcement, and placing of reinforcement.

2.3 Examples of using GPR for scanning of concrete structures

According to (Benedetto & Pajewski, n.d.) Ground Penetrating Radar (GPR) has well established use in civil engineering and have wide range of applications in locating the buried services like tunnel structures, detecting of voids and cavities, reinforcement mapping and location, investigation of geological foundations, archeological surveys, environmental and hydro-geological surveying. GPR applications in civil engineering field are described as following:

2.3.1 Depth determination

According to (*Concrete Scanning with GPR Guidebook*, 2015) to obtain the accurate depth measurement correct concrete type (Velocity) is required. Fluctuation in velocity happens due to diversity in aggregates and water content in concrete. Tight hyperbolas give the accurate location of the object and depth detection. To get accurate shape of hyperbola and depth determination target should be crossed at 90 degrees by GPR. Due to incorrect calculation of velocity hyperbola shapes get distorted.

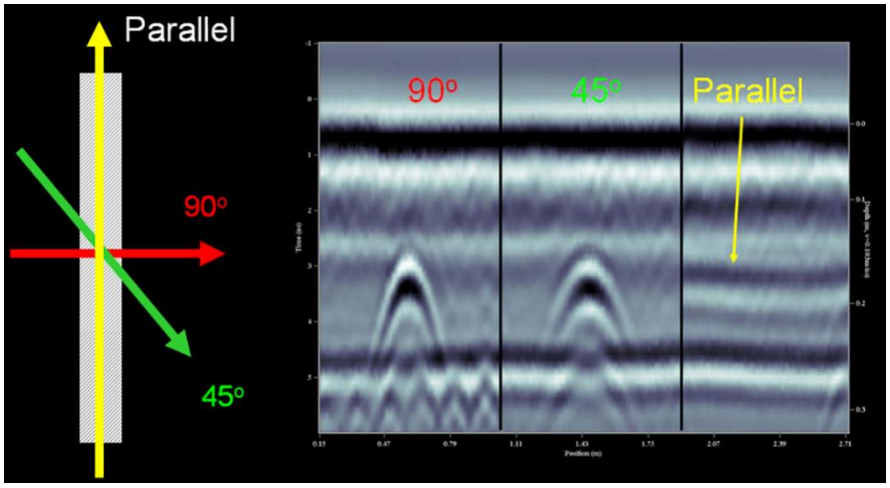

Figure 24- Cross the target at 90 degrees to generate the "tightest" (*Concrete Scanning with GPR Guidebook*, 2015)

(Wiwatrojanagul et al., 2017) tried to determine the buried object's diameter and concrete cover thickness from experimentally obtained GPR data form different concrete specimens with embedded steel rebars and steel pipes. Proposed method developed based on modification of existing hyperbolic signatures by (Al-Nuaimy et al., 2000) to make if efficient in the detection of buried objects and cover thickness estimation. According to comparison of results from new and existing hyperbolic data average accuracy in cover thickness was found to 3.12%. It showed that proposed method is highly accurate than the existing model.

(Zhou et al., 2018) says that by knowing the EM wave velocity of the GPR signal, concrete cover thickness can be estimated by hyperbolic apex cone. Determination of EM velocity is difficult task due to heterogeneous properties of concrete material and having different dielectric constants. A conic equation was developed regarding reinforcement diameter, concrete cover thickness and EM velocity in concrete and fitting between extracted trajectory of rebar reflection and modelled hyperbolic curve for estimation purpose of diameter of rebar, cover thickness and velocity of EM wave.

2.3.2 Defect detection (honey combing and foreign objects etc.)

It is challenging task in inspection of concrete structures to detect and characterization of honeycombs and voids. Due to variability in the size, shape, position, orientation, and density it is challenging task is detection and recognition. Honeycombs are different than voids create gradual and volumetric distributed change in material properties, that's why direct detection is not possible and multi sensor investigation is required for that purpose (Völker & Shokouhi, 2015).

From last 20 years GPR system has been used for the investigation and inspection purposes of concrete structures. According to GPR working principle, transmission of EM waves and signal attenuation of reflected EM waves from the encountered objects depending on different dielectric properties. Reflece3td signals are interpreted to evaluate the subsurface properties and size of encountered objects. (Tosti & Ferrante, n.d.) provided literature about GPR systems used for the investigation purposes of the reinforced concrete structures. In GPR system three different approaches are used for investigation and inspection purposes as following:

- Within default frequency range of transmitting radar, frequency modulation continuous frequency
- Use of synthetic pulses over a series of discontinuous steps with variable frequency of transmitted signals
- Impulse radar-based system

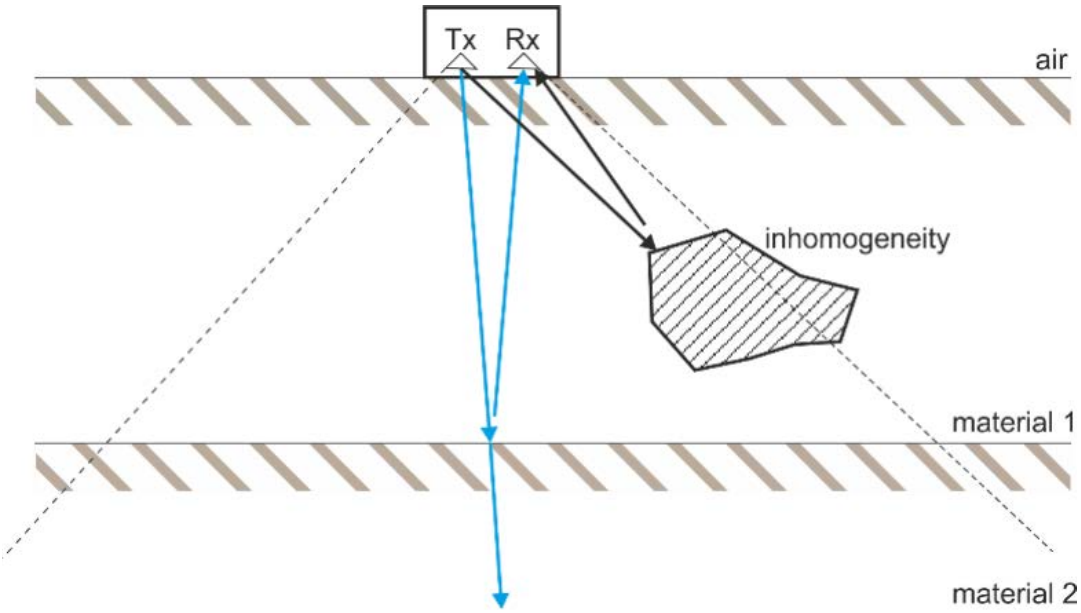

Figure 25-Investigation of a subsurface anomaly using a GPR ground-coupled antenna system (Tosti & Ferrante, n.d.)

(McCabe et al., 2021b) evaluated the GPR system's possibility and effectivity of honeycombing detection during construction in a concrete pavement. GPR has been used for quality control and delamination detection since 1980s. this project includes the preliminary field testing on concrete pavement using GPR to check possibility of honeycombs detection and investigation of concrete specimens with embedded artificial voids of different shapes and sizes for detection purpose with high frequency GPR antenna. According to field and lab experimental results, GPR is an effective tool for investigation of air voids and honeycombs. research is concluded that GPR can detect air voids or honeycombs in the size range of 3.8cm to 10.16cm in concrete pavement within three hours after placement of concrete.

Since from 1980s GPR can detect voids in the subsurface of concrete and estimation of concrete cover depth according to (Al-Qadi et al., 2003) due to easy use and mobile nature in processing.

(Cassidy et al., 2011) performed a comparative study of GPR and ultrasonic pulse for detection of steel reinforcement and voids in concrete structures along with their subsurface location.

According to (J. Liu et al., 2008), GPR having unique ability in evaluation of substructure conditions make it usable for detection of shallow delamination in continuously reinforced concrete (CRC). High frequency ground coupled GPR found effective in mid slab delamination detection, location of steel reinforcement and subsurface defects like air voids and rock pockets.

2.3.3 Locating and mapping of reinforcement bars

(Soldovieri et al., 2006) proposed a study of inverse scattering approach for detection of reinforcement location automatically. Authors got success with application of specific algorithms to GPR in situ data to obtain tomographic images of the structures. A mesh of deep and shallow reinforcement was obtained in the topographical images of concrete structures.

(Hugenschmidt et al., 2010 performed an experiment on retaining wall with two reinforcement layers using antennas in two orthogonal directions for investigation purpose. GPR dataset was processed using 2-D processing leading 3-D data cube leading data fusion and inverse scattering by followed by data fusion. Using above mentioned approach complete map of both horizontal and vertical reinforcement is obtained for top rebar layer. For 2nd layer lower quality results were obtained.

3 Methodology and GPR measurements

This chapter describes the experimental work done for data collection from 3 different concrete structures to characterize using GPR. The three different testing structures are thick concrete wall, a reinforced concrete retaining wall and precast concrete slabs. It includes the scanning process, objectives, and description of the scanned area. Experimental work includes the scanning of the three different type of concrete structures as described below. Used GPR for experimental work is PS 1000 X-SCAN CONCRETE SCANNER manufactured by HILTI shown in the following *Figure 26*.

Figure 26-PS-1000 X-Scan Concrete Scanner

Specifications of PS-1000 X-Scan Concrete Scanner are described below

- Maximum detection depth of the GPR is 300mm for localization of the objects in the concrete structure.
- Accuracy of depth indication: <100 mm: ±10 mm, >100 mm: ±15 %
- Instrument localization accuracy is ±10 mm

GPR principle, structure and components of the instrument are described in chapter 2, here working, and used methodology is described. This instrument provides 3 types of scanning (1) QuickScan detection, QuickScan recording and image scan detection.

Quickscan detection is used to indicate the objects in concrete directly during scanning and objects lying perpendicular to the scan direction becomes visible on plan or cross-sectional view and can be marked directly on the surface.

Quick Scan recording is used to scan the longer path on the concrete structure, at the end of scanning perpendicular objects to the scan become visible in the recording in plan view or cross-sectional view.
Imagescan function provides the image of the objects present in specific area. These objects are shown in plan and cross-sectional view. In this thesis imagescan option is used for scanning purpose of the concrete structures.

3.1 Measurements on thick-walled reinforced concrete wall and foundation

Thick mock concrete wall and floor dimensions are in the Table 1 & 2. Wall has three sides A, B and C to distinguish the GPR images and scans and references.

3.1.1 Objectives of the investigation

Main objective of investigation was to determine the porosity of the concrete wall using GPR images and scans, GPR scans of concrete wall aren't good to determine the porosity of the concrete wall and to characterize accordingly. Maximum scanning depth of used GPR is only 300mm and it is unable to detect and scan the whole thickness of the wall from each side. Following are the objectives of the investigation.

- Find and locate the hidden objects in the wall, location, and determination of the embedded defects in the concrete wall
- Reinforcement mapping of the wall
- Checking diameter of rebar if possible
- To determine the concrete cover thickness of the wall
- Find and locate the hidden cracks/internal defects (Construction defects) in the concrete wall

3.1.2 GPR scanning procedure of the wall and data acquisition

GPR scanning procedure is followed from the (HILTI) as following for all objects under experiments.

1- Reference grid is placed on the surface to be scanned at right angle in the direction of objects orientation and fix it to concrete surface using adhesive tape. To make sure that the distance of reference grid and scanner display distance are accurate the reference grid should be tightened and flat on the surface to get effective results.
2- Choose imagescan option for the menu of the scanner.
3- Select grid size form the menu corresponding to the reference grid attached to the surface. possible grids with PS-1000 are 600*600 and 1200*1200.
4- Hold the scanner against surface of the area to be examined at the starting point and in line with the grid. By pushing start/stop button

scanner starts with a beep and double beep indicate the end of path under scanning. The scan ends automatically at the end of each path.

5- Scan all the paths according to grid and speed of scanner movement should be in the limit and if moving speed is more than a maximum approach, repeat the scan. On display scanning process is indicated by the bar, red bar turns into black when minimum length is reached.
6- Previously scanned paths can be discarded by pressing “Cancel” button and new scan can be started, when last path has been scanned result is displayed immediately for checking and evaluation.
7- The “Contrast”, “Param.” and “Visualization” buttons are used to change the visualization and calculations parameters, by changing the parameters data must be recalculated, to do this press OK button.

From above mentioned procedure scans are obtained from the wall and foundation of the wall which is also refereed as floor. Obtained scans are analysed and visualized using the software PROFIS DETECTION OFFICE. Scans are stored in the memory card installed in the instrument and then that data is transferred to the computer to analyse with the help of detection software. Data is imported to the software to get analysed and to obtain the results. User interface of the software is shown in the following *Figure 27*.

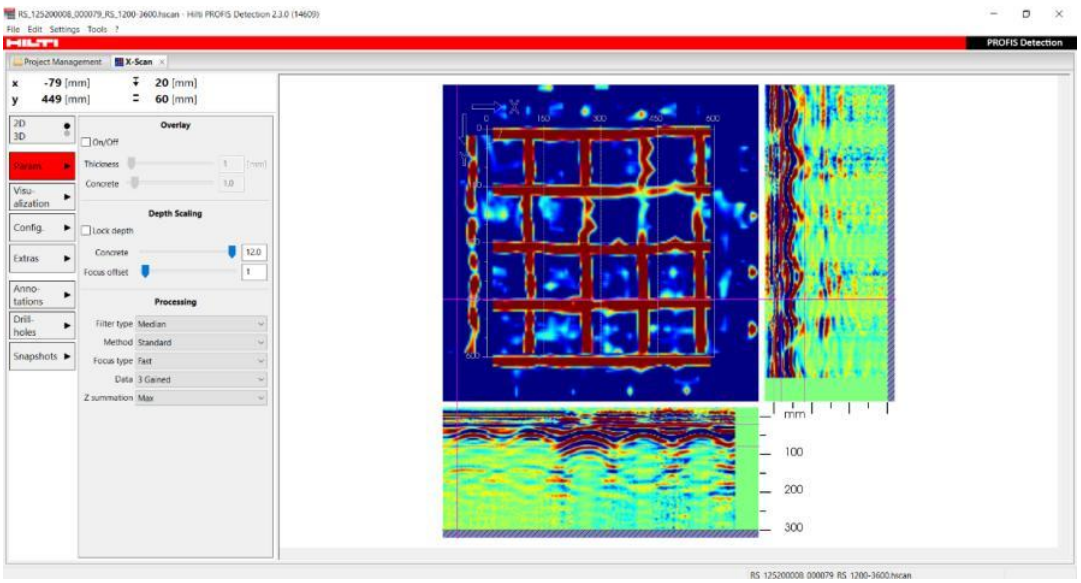

Figure 27- User Interface of Profis Detection Software

There are 8 different functions including 2D and 3D view of the scan, different parameters for analysis of the scan, configuration for setting different colour schemes of the scan, extras to report generation, to edit the coordinates and preview icon of the scan, annotations for marking the location of objects on the scan, drill holes to embed the holes in the object and snapshots to store the snaps during analysis. Parameters button provides the overlay option, depth scaling for concrete and focus offset and processing column to

process the scan using filter type, method, focus type, data, and z summation to analyse the scan with different and iterative functions. For analysis of GPR scans in this thesis work used parameters for processing of the scans are following:

Filter Type has three different options: selective, median, and high pass. Median option is used to have better view and to get effective details form the scan.

Method has two options: standard and advanced. Advanced option is used for the processing of scans as it provides the whole view across thickness of the objects and small objects are visible like voids and small cracks.

Focus Type has two options: Fast and advanced, Fast option is used as it give the more clearer and bright details than advanced option provides the blurry view of objects.

Data is set to default option to have a clear detail of the hidden objects in the cross-sectional views.

Z Summation is the depth of the scan and is kept at maximum level within the penetration limit of GPR scanner i.e., 300mm.

Using visualization button contrast scheme can be altered for 2D and 3D view of the scan for effective visualization. GPR scans are analysed using contrast slider from lower to higher percentage to check all the minimal details of the scans. Visualization function provides the cross-sectional details of the object and cross hairs to move around the cross section to view different objects and different locations in the main view of the scan. It offers also the three different faces of the view for 3D cross sectional view. In configuration option we can check the scan data and details in horizontal and vertical cross-sectional views of the object and can hide unwanted details of the scan.

3.1.3 Description of the scanned area

Thick concrete wall is constructed in Aalto University in the backside of School of Civil Engineering (Rakentajanaukio 4, 02150 Espoo) for investigations purposes using NDT & E methods and techniques .Dimensions of the wall and floor base are mentioned in Table 3 & Table 4. Thick concrete mock wall has simulated defects during construction of the concrete wall and base. As we know common concrete occurring problems during the use of the concrete structures are defects, damage, and deterioration. Defects could be in construction, design, and during construction. Concrete damages are classified as overload, fire, impact loading and chemical spill. Deterioration effects are metal corrosion, erosion, freeze and thaw, sulphate attacks and time dependent changes in the chemistry of the concrete. To determine all possible concrete defects and damages, thick mock wall and base is embedded with simulated defects like delamination, air filled voids, water filled voids and honeycombing and cracking as shown in *Figure 18*. Purpose of the floor base of

slab base is load transferring of mock up wall to soil and for semi destructive testing and drill sampling to evaluate the concrete quality (Al-Neshawy, Ferreira, et al., n.d.). Mock up wall is reinforced with three different types of reinforcement as shown in *Figure 19*.

- Conventional reinforcement having different density in two different areas of the wall
- Steel lined in one side of the wall
- Prestressed tendon ducts

Mock up wall and slab are embedded with simulated defects/ foreign objects as shown in *Figure 18*. Foreign objects/ simulated defects are:

- 05mm thick plastic sheet and 0.25mm thick cloth squares are used for detection purpose of delamination
- Air filled voids are simulated using insulation of foam squares of 13mm thickness in vacuum seal
- Water filled voids using water filled bags in vacuum sealed plastic bags
- Honeycombing and cracks
- Duct grouting defects (Al-Neshawy, Ferreira, et al., n.d.)

Table 3- Mock Wall Dimensions

Dimensions	Size (mm)
Width	1000
Length	3500
Height	2000
Volume	7000 (mm^3)

Floor area is the base of the concrete wall having the following dimensions:

Table 4- Wall Base (Floor) Dimensions

Dimensions	Size (mm)
Width	3000
Length	5500
Height	400
Volume	6600(mm^3)

Figure 28- Schematic overview of the thick-walled concrete structure(Al-Neshawy, Ferreira, et al., n.d.)

Three side of the wall are nominated as Side A, B and C as shown in the figure.

Figure 29- Three Sides of Concrete Mockup Wall

3.1.4 Description of the scanning process

Wall has three sides A, B and C shown in figures. Dimensions of the wall and floor are given in the Table 3 and Table 4. Scanning of three sides of the wall and floor is done as following.

Side-A

Side A is cleaned with brush to remove the dust particles and leaves for the area to be scanned and then reference grid is chosen according to the dimen-

Figure 30- Scanning of Side-A

sions of the side A. As side A is 1000mm wide and 2000 mm high, so small reference grid of size (600*600) is attached to the wall as shown in *Figure 30* using the adhesive tape and made it tightened from all side to get the better view in the scan display. Starting and ending point of the scan are marked on the wall using permanent marker to get the starting reference of another scan if needed.

In the GPR, a project is created, selected aligned grid size and image scan option is selected to have the scan of side A. Scanner is put on the starting point, pushed the start button on the handle and moved it according to the display on the screen for each grid to have a full image of the area (600*600). After completion of the 1st scan, reference grid is removed and attached again on the unscanned part starting from 600 mm. Following the same procedure 2nd scan is obtained from the wall.

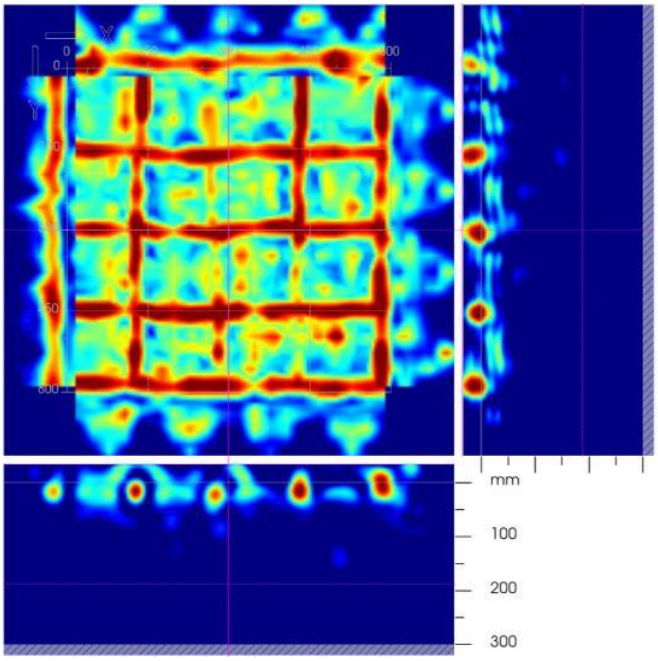

Figure 31- GPR Scan of Side -A

Two GPR scans of the wall side-A are shown above. *Figure 31* is showing 1st scan having coordinates (0,600) (600,600) and 2nd scan coordinates are (600,600) (600,1200). It shows that scanned area for the side A is (600*1200) mm².

Side-B

Side B of the wall is 2000mm high and 3000mm wide according to Table 4. Reference grid of size (1200*1200) is chosen to cover the maximum area of the wall in a smaller number of scans. Reference grid is attached to wall as shown in *Figure 32* with the help of adhesive tape and starting and ending points are marked on the wall through the holes on those points. Using Grid size of (1200*1200) scan is obtained from the wall. As wall height is 2000mm and was unable to scan the area below the first scan using the reference grid (1200*1200), that part is skipped and next scan was started from (1200, 1200) coordinates and ended at (2400, 3600) coordinates and scans are named according to the reference grid coordinates. Scanned area of Side-B of the wall is (1200*3600 mm²)

Movement of the scanner is very important to take care to get the good quality scans. As GPR scanner must be moved along the direction of grid and be within the size of the horizontal and vertical grids. After visualization of scan from the instrument, can be retake scan in case of any ambiguity. From side -B only two scans are obtained.

Creating different project in the GPR scanner and scans are named according to the coordinates on the wall.

Figure 32- GPR Scanning of Side-B

One of the obtained scans form the Side-B is shown in *Figure 33* showing the rebar mapping and location of the rebars can be seen from the cross-sectional view of the GPR scans.

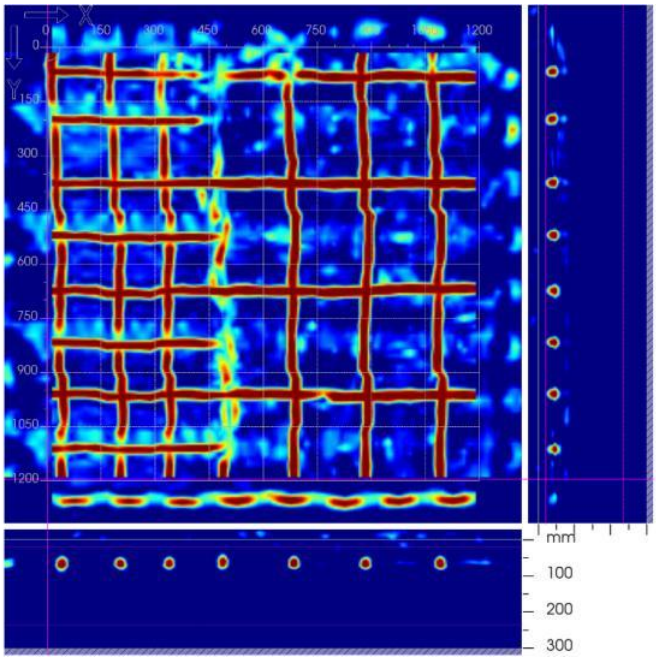

Figure 33- GPR Scan of Side-B

Side-C

Side C dimensions are same as Side A, so same reference grid of (600*600) is used for the scans and two scans are obtained from that side covering area of (600*1200). *Figure 34* shows GPR scan of Side-C with rebar mapping and cross-sectional details.

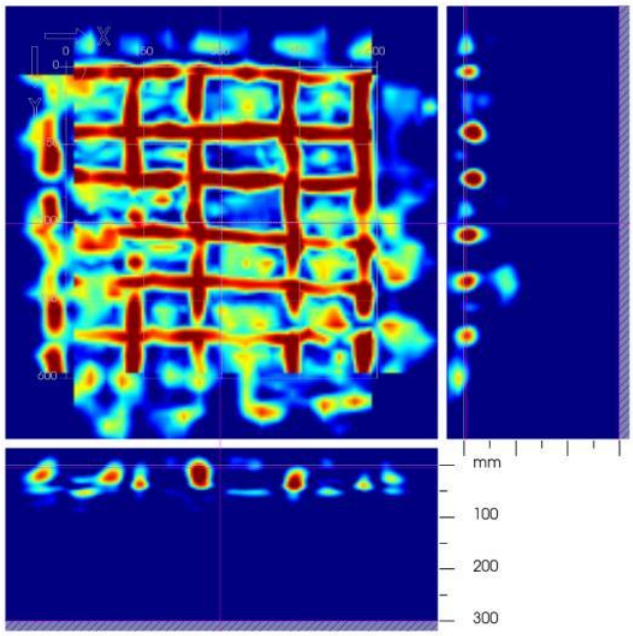

Figure 34- GPR Scan of Side-C

Floor (Wall Base Slab) Area

After scanning of the three sides of the wall floor base is scanned using the same procedure. Floor is extended 1000mm from all four sides of the wall and using reference grid of (600*600) is used to obtain the scans of the floor. Floor area of the concrete wall is scanned in 20 scans. Starting point of the scanning is left corner of the side A of the concrete wall. As it was not possible to scan the edges and corners of the floor with wall using GPR, transmitters downside of the instrument must move on the surface to get the scans so leaving some feasible distance from the edges of the wall scans are obtained from the floor surface. A numerous number of scans are obtained to cover the whole floor area. One of the GPR scans for the floor is shown in *Figure 35*.

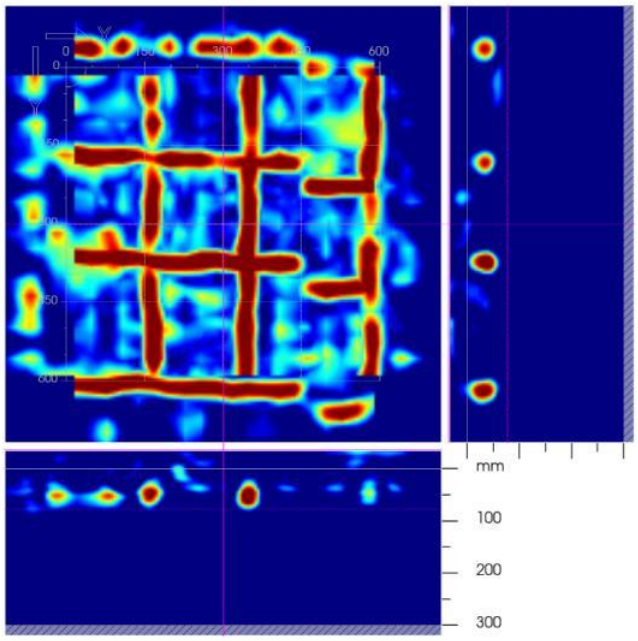

Figure 35- GPR Scan of Wall Base Slab

3.2 Measurements on reinforced concrete retaining wall

Reinforced concrete retaining wall is constructed to retain the uphill soil in the backside of Undergraduate Centre (Otakaari 1d, 02150 Espoo) as shown in *Figure 36* . Wall measurements are taken by visual estimation and design data is not available.

3.2.1 Objectives of the investigation

Objectives of the retaining wall scanning are following.

- Find the thickness of the retaining wall
- Location of the visual and internal cracks from the GPR scans
- Location and mapping of the reinforcement in the wall
- Find and detect the internal defects in the concrete wall
- Diameter of the rebars if possible

3.2.2 GPR scanning procedure of the wall and data acquisition

Scanning procedure for the retaining wall is same as for the thick concrete wall, GPR scans are obtained and analyses using the Profis Dtection Software for investigation of the retaining wall.

3.2.3 Description of the scanned area

Figure 36- Reinforced Cocnrete Retaining Wall in Aalto University

Dimension of the retaining wall are roughly estimated mentioned in Table 5.

Table 5 - Assumed diemnsions of Reinforced concrete retaining wall

Height	7 feet (2133mm)
Scanned Length	4800mm
Thickness	200mm

Scanned area of the retaining wall is chosen including the visual cracks on the wall and some environmental defects like erosion, abrasion, and small cracks in the wall throughout the depth of the wall as shown form the *Figure 37*. There are aging effects on the wall and due to heavy moisture and humid weather there is algae and a layer of brownish and blackish residues growing on the wall.

Figure 37- Visual detail of cracks and environmental effects on reinforced concrete retaining wall

3.2.4 Description of the scanning process

The purpose of the scanning is to include all the visual cracks and defects in the GPR scans. Wall was cleaned using brush to remove the dust particles and aging residues like algae spores. Area of the wall is marked for scanning including all the visual cracks and defects seen with naked eye. After marking the area to be scanned reference grid of size (1200*1200) is attached to the wall from the starting point using adhesive tape to stick to the wall and graph is tightened to get the good scans aligned with the instrumental grid size. Choice of grid size depends upon the area to be scanned as for bigger area

reference grid is selected big and vice versa. One of the four scans is shown in *Figure 38*. Scanned area of the wall is 1200*4800 mm².

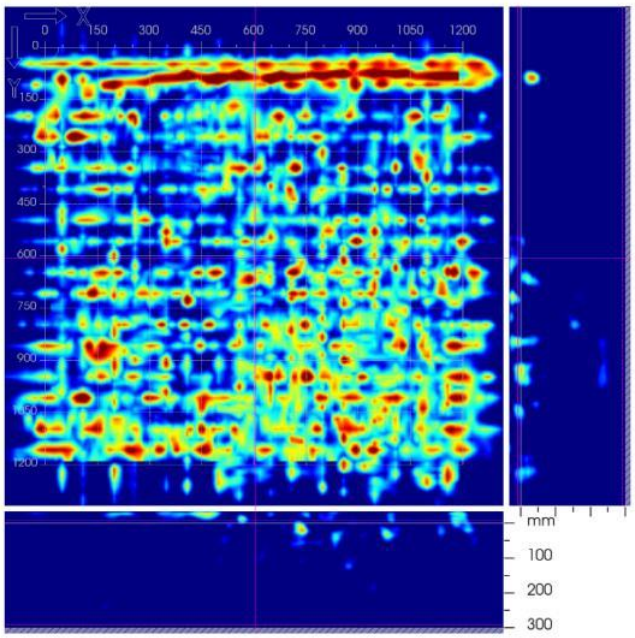

Figure 38- GPR Scan of Reinfoced concrete retaining wall

3.3 Measurements on reinforced concrete slabs

Precast reinforced concrete slabs are scanned using the GPR as following.

3.3.1 Objectives of the investigation

Investigation objectives of the reinforced precast concrete slabs are following:

- Location and mapping of the reinforcement in the concrete slab
- Cross checking the diameter of the premade holes in the slab and diameter of the rebars in the concrete slab
- Detection of the possible defects and foreign objects in the reinforced concrete slabs

3.3.2 GPR scanning procedure of the slabs and data acquisition

Same procedure as mentioned in 3.1.2 is followed for the scanning of precast reinforced concrete slabs.

3.3.3 Description of the scanned area

There are two precast reinforced concrete slabs named as Slab-1 and slab-2. There are premade holes in both slabs for the design purpose and these holes are not symmetrical locations on the slabs. Slabs and GPR scanning of precast slabs are shown in *Figure 39*.

Figure 39- GPR scanning of Precats Reinforced Cocncrete Slabs

3.3.4 Description of the scanning process

Two projects with the names of Vantaa Slab-1 & Vanta Slab-2 are created in the GPR instrument to differentiate the scans. After removing the dust particles from the slabs grid reference is kept on the slabs to get scans. Size of the grid is chosen (600*600) from instrument keeping in view the dimension of

the slabs. Scanning process can be seen form *Figure 39*. 3 GPR scans are obtained from each of the precast concrete slabs. GPR scans from Slab-1 and Slab-2 are shown in *Figure 40* & *Figure 41*.

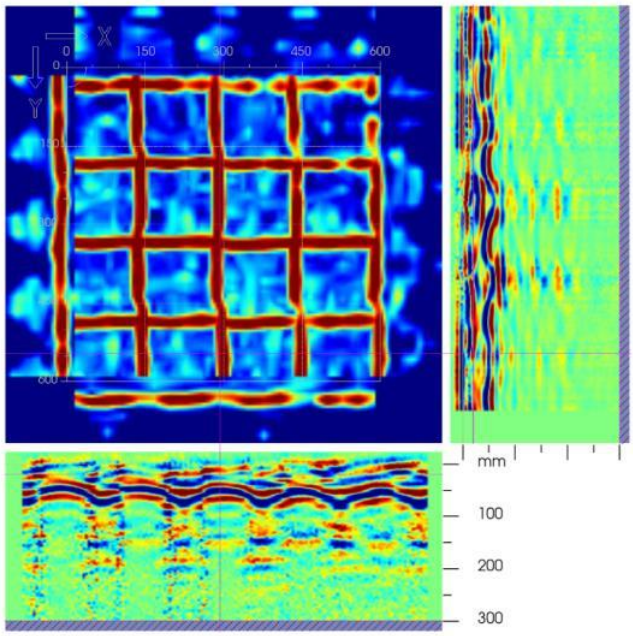

Figure 40- GPR Scan of Slab-1

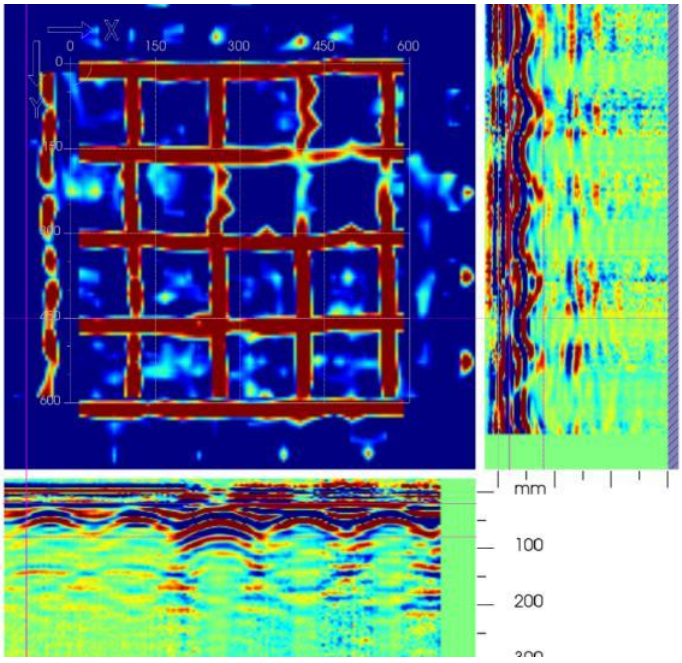

Figure 41- GPR Scan of Slab-2

4 Data analysis and discussion

This chapter presents the data analysis and discussion about the investigation and inspection of the concrete structures using GPR. Approach of analysis is divided in two types, in first approach using the 2D scan, detection and location of hidden objects is tried to define and using 3D view analysis, location of different objects, defects and foreign objects are located and defined throughout the penetrable depth of concrete which is 300mm.

4.1 Investigation of thick reinforced concrete wall (Mockup Wall) and Wall Base Slab (Floor)

Thick reinforced concrete wall has foreign objects embedded in the wall and there is a pipe throughout the length of the wall and in the center of the wall in wide direction. Aim is to find the location of the pipe and detection of the embedded objects for the GPR scans. According to objectives of the investigation analysis and investigation of the wall is done as shown in the following figures. Wall has three sides and foundation which is also called base floor of the wall. Using Profis detection software scans are investigated with 2D and 3D views. GPR scans of the three sides of the wall are evaluated and inspected as following.

4.1.1 Data acquisition for GPR imaging and mapping of the internal defects

GPR images of the three sides of the wall are analyzed using Profis Detection Software by HILTI.

Side-A

GPR images of Side-A of the concrete wall are analyzed with 2D and 3D visualization as following. First 2D scans are briefly explained and detected objects are notified. 1st scan of the wall has coordinates (0,0) (600,600) and analyzed by keeping the depth or cut off thickness of the concrete is 300mm as penetration depth of the GPR scanner is 300mm.

Figure 43 shows the arrows directed to the deflected EM wave which tells the location of the rebars which is 50mm from the top surface of the wall. Location of rebars form the top of the concrete surface, concrete cover thickness can be assessed easily. Concrete cover thickness is around 50 mm as shown in the scan of the wall. Location of the reinforcement talks about the thickness of the concrete cover, and it seems the thickness of concrete cover is about 50mm.

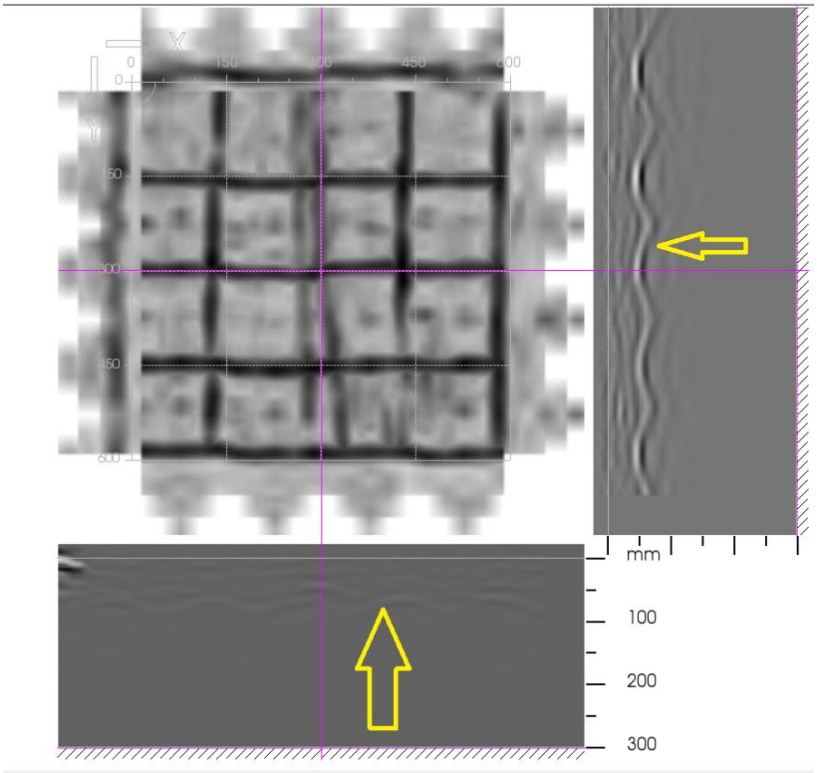

Figure 43- Location of Rebars and Estimation of concrete cover depth using hyperbola curves from GPR 1st Scan of Side-A

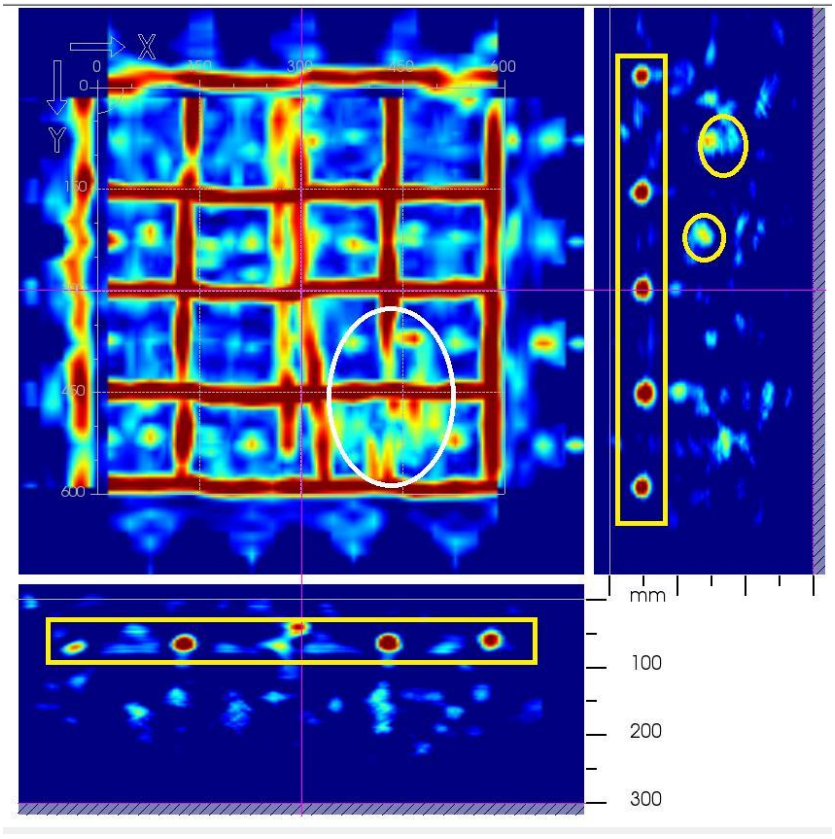

Figure 42- Rebar Mapping and detection of anomalies form GPR 1st scan of Side-A

From *Figure 42* rebar mapping and rebar spacing can be seen. Rebar spacing is 150mm and rebar diameter can be assessed from the grid spacing as spacing between the grids is 150mm and rebar is occupying 1/6th of the total space and we can say that diameter of rebar is around 25mm as seen from the GPR scan. Horizontal and longitudinal reinforcement is shown in the cross-sectional details of the scan. White circle in the figure shows the discontinuity of rebars and can be said that rebar is broken or rusted from that location. If we see in the middle of the scan, there are two rebars are shown adjacent to each other. One is the main bar/reinforcement and other one looks a pipe or thick electrical wire, can be confirmed from the original design of the wall as there are some foreign objects are installed by purpose during the construction of the wall. From cross sectional views vertical and horizontal reinforcement is shown and two objects are circled. Circled objects are hard to define and can only be said that those are voids or smaller objects. There are small green chunks are shown at the bottom side of the cross section, those can be voids or capillaries in the wall at that location.

3D Scan:

Figure 44 is 3D scan of the 1st scan of wall side-A. From 3D scan rebar map is shown clearly and smaller objects are included in the yellow rectangle to imagine the depth and location of the voids and smaller metal objects.

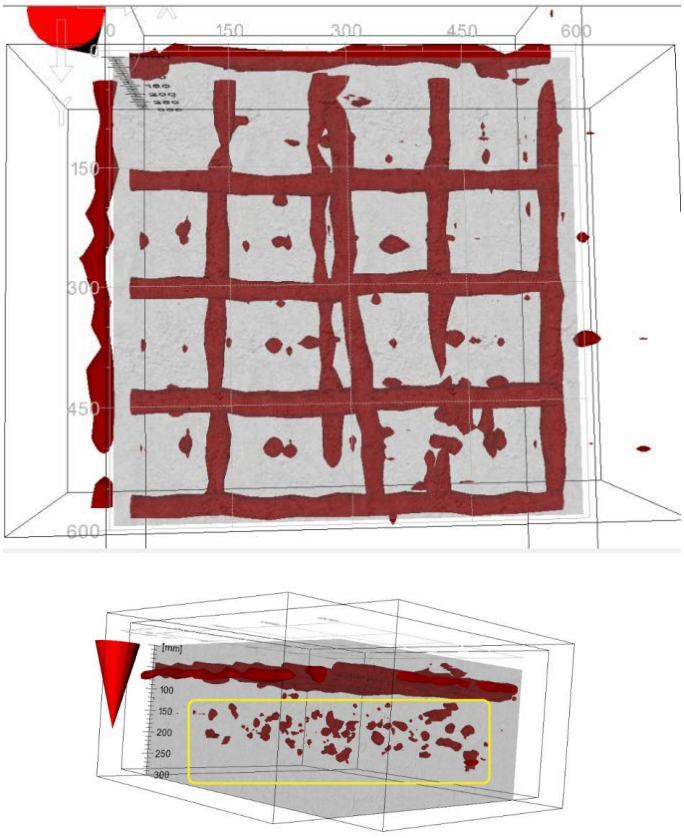

Figure 44- 3D view of 1st scan of Side -A showing the rebar details and other metallic object or voids

Figure 45 is the 2nd scan of the wall side A, and we can see the location of reinforcement directed by the yellow arrows in the filtered view of the scan. The reinforcement location is 50mm from the top surface of the concrete wall, which also tells about the concrete cover thickness of the wall that is equal to 50mm. We can see the deflected wave location that is exactly at 50mm from the top of the surface.

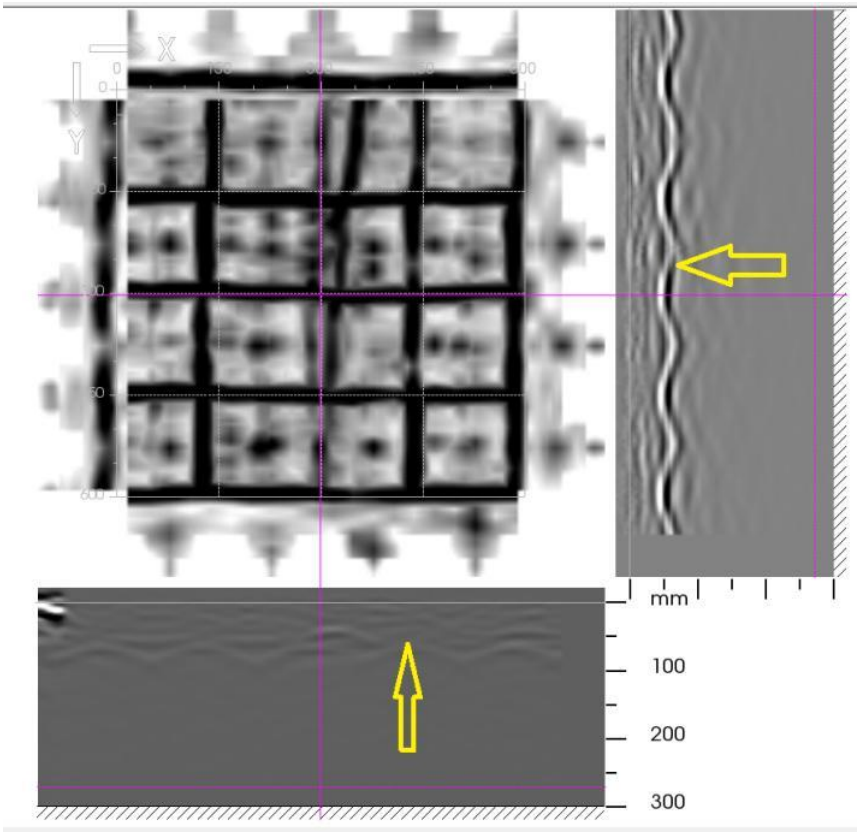

Figure 45- Location of Rebars and Estimation of concrete cover depth using hyperbola curves from GPR 2nd Scan of Side-A

Figure 46 shows the rebar mapping and detection of different objects. From rebar mapping, spacing between rebars can measure 150mm as rebars are exactly located on the grid lines. Some objects in the cross-sectional details are circled, such as voids or small metal objects in the concrete wall at that specific location. The cross-sectional view shows the horizontal and vertical rebars, and the diameter of the rebars is about 25mm, as assessed from the 1st scan of this side of the wall. In the middle of the scan, two red lines overlap each other, and one of them is rebar, and the other one could be a rebar, pipe or metal wire running throughout the height of the wall.

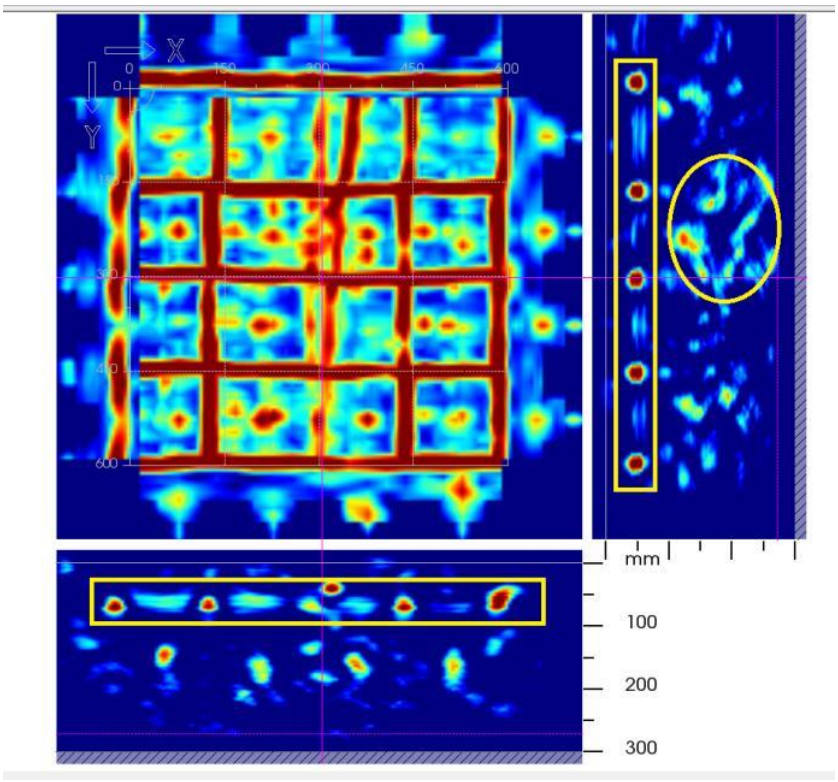

Figure 46- Rebar Mapping and detection of anomalies form GPR 2nd scan of Side-A

From the 3D view of the scan, only the rebar map is visible as already detailed based on the 2D scan, and there are some smaller objects scattered in the whole area of the scan but at the same location as the rebar map, like in the depth range of 50 to 100mm. Four objects in the vertical direction in the scan at the location of 420mm, can be said to be different objects or cavities in the concrete wall. By the object smoothing option, two fine lines are shown at the bottom of the area, and it can be said easily that these could be cracks or thin steel wires in the wall at that specific location, as shown in Figures & *Figure 48*.

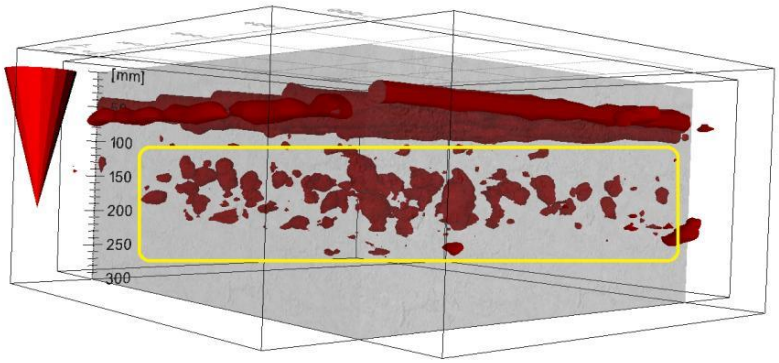

Figure 47- 3D view of 2nd scan of Side -A showing metallic object or voids

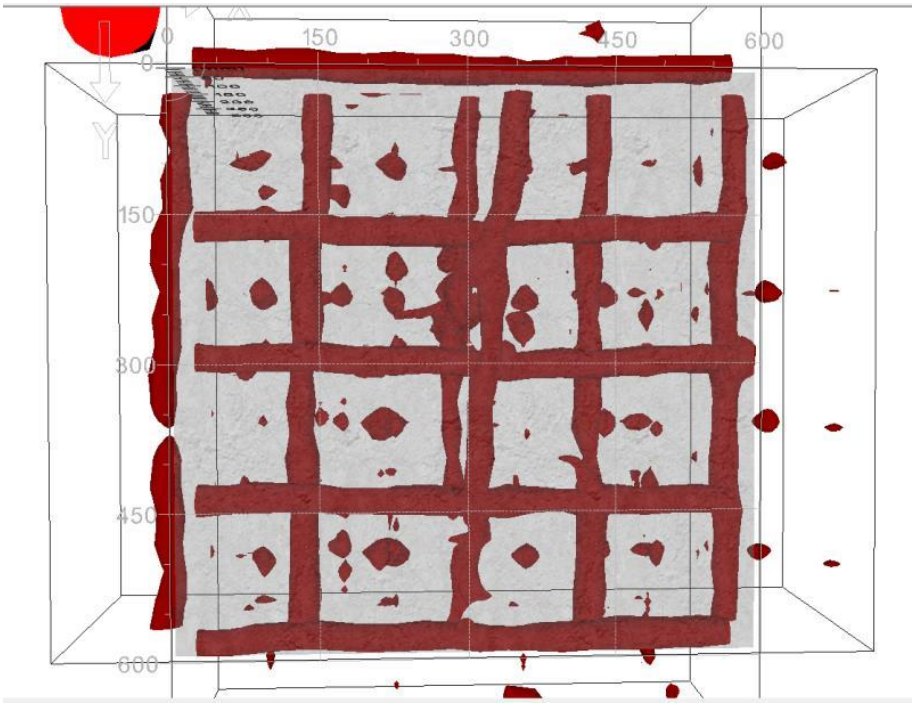

Figure 48 - 3D view of 2nd scan of Side -A showing the rebar details

Side B

Figure 50 shows the 1st scan of the thick concrete wall from Side-B having coordinates (0,0) (1200,1200). The thickness of the wall from that side is 1000mm, and the penetration depth of the scanner is only 300mm, so from Side -B, we can only see the wall details until 300mm. Figure 30 shows the location of the reinforcement from the top surface of the concrete wall. The deflection of EM waves detects the location of the reinforcement, as shown in the figure with yellow arrows. The reinforcement location is almost 50mm from the top surface of the concrete wall; hence, the concrete cover thickness of the wall is 50mm.

Figure 49 shows the rebar mapping and the location and depth of different objects in the scanned area of the wall. From rebar mapping, rebar spacing is equal to 150mm. The reinforcement map shows the discontinuity at two locations in the scan, 600mm and 900mm. The discontinuity can be a human error in the scanning procedure. From the cross-sectional details, horizontal and vertical rebars are shown, and some detected objects are circled. Circled objects are located at a depth of 200mm from the top of the concrete surface. The rebar diameter is assessed as 25mm, 1/6th of the grid spacing. Two metal objects are visible at a depth of 200 from the face of the wall location of 600mm from the start of the scan and 75mm from the top of the scan. There are two objects in the horizontal direction at 450mm and 750mm, as shown in Figure 31. Using 50% contrast, numerous metals and other objects are

visible at a depth of 200mm in the thickness of the wall. Objects with blue colour could be internal cracks or voids in the concrete wall, and red objects

are metal pieces in the concrete wall at the thickness of 200mm from the side B of the concrete wall.

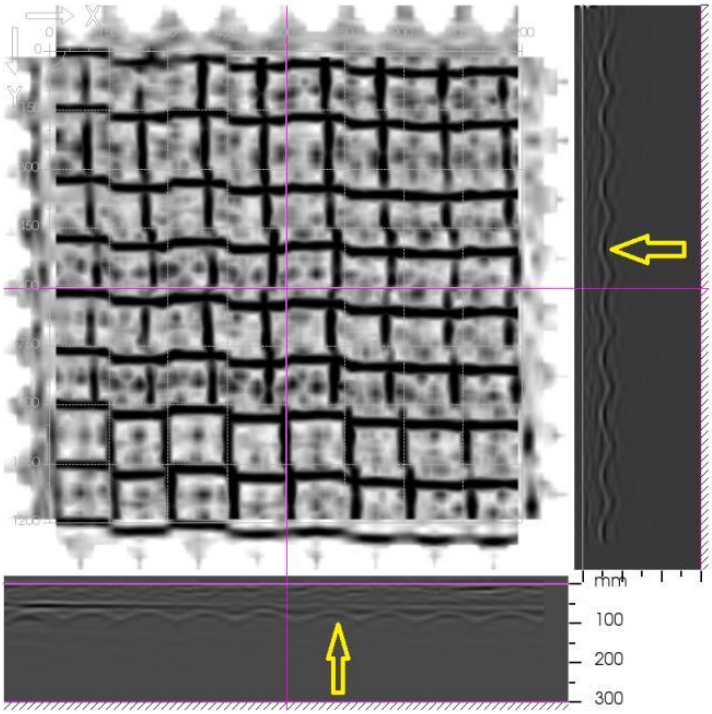

Figure 50-Location of Rebars and Estimation of concrete cover depth using hyperbola curves from GPR 1st Scan of Side-B

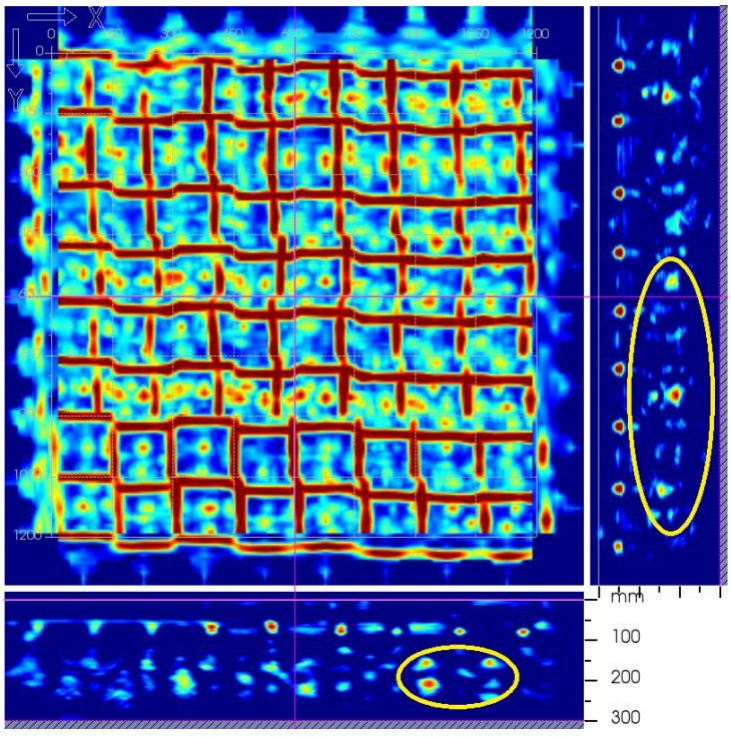

Figure 49-Rebar Mapping and detection of anomalies form GPR 1st scan of Side-B

Figure 51 is 3D visualisation of the 1st scan of the side B of the wall showing the reinforcement mapping and detected objects at different locations in the scanned area of the wall. From a 3D view, the location of the objects in the concrete layer of 300mm is also cleared.

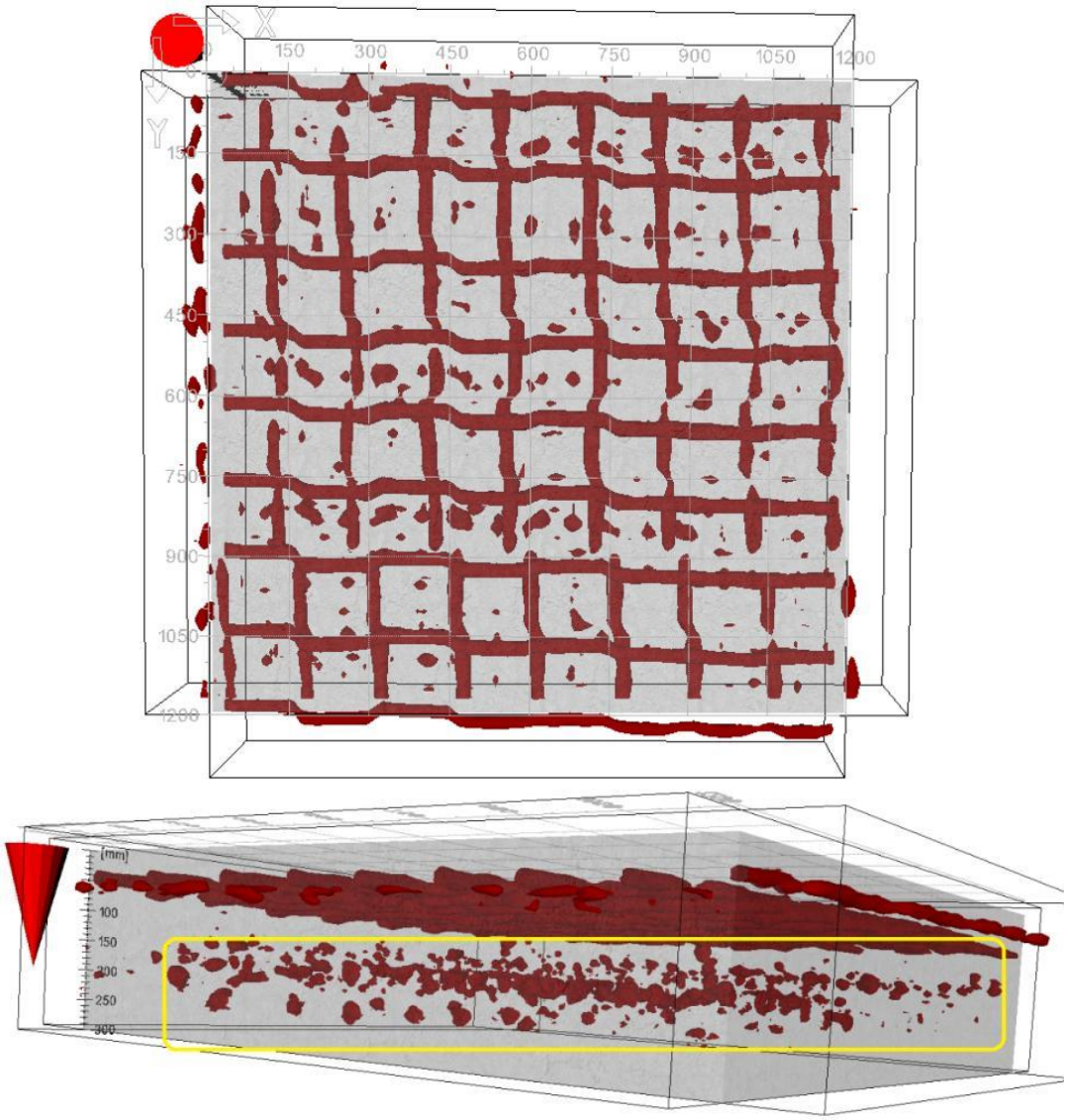

Figure 51- 3D view of 1st scan of Side -B showing the rebar details and other metallic object or voids

Figure 52 shows the 2nd scan of Side B of the concrete wall. The coordinates of the GPR scan are (1200,0) (1200,2400), obtained right next to the 1st scan of the wall. Shows the location of the reinforcement at 50mm from the top surface of the wall. It also means that the concrete cover of the wall is 50mm. *Figure 53* shows the rebar mapping and location of different objects detected by the GPR in the scanned area of wall side B. At the location of 450mm in the horizontal direction of the scan, there is a scattered rebar or metal object, which makes a partition between the closed-spaced reinforcement and wider

space reinforcement on the other side. It can be seen from the figure that on the right-side horizontal bars are more widely spaced than on the left side. Circled rebar is located at a depth of 200mm from the top of the wall surface.

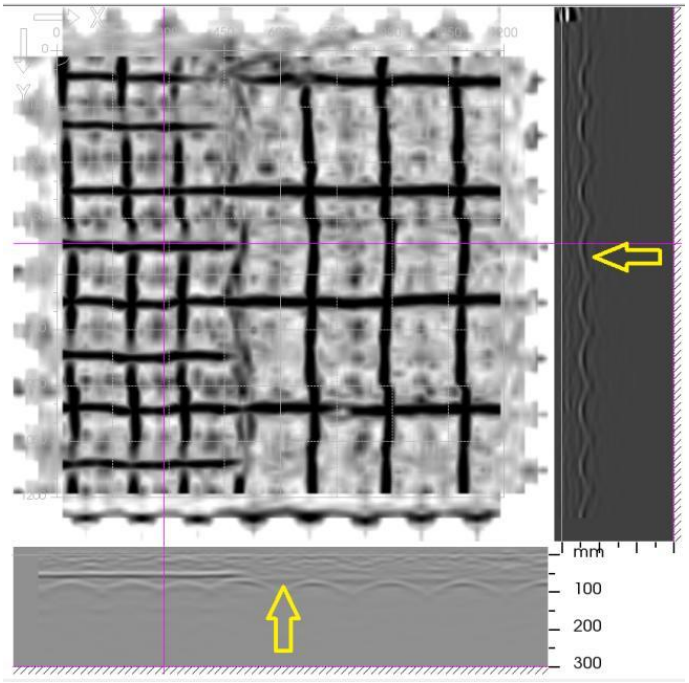

Figure 52-Location of Rebars and Estimation of concrete cover depth using hyperbola curves from GPR 2nd Scan of Side-B

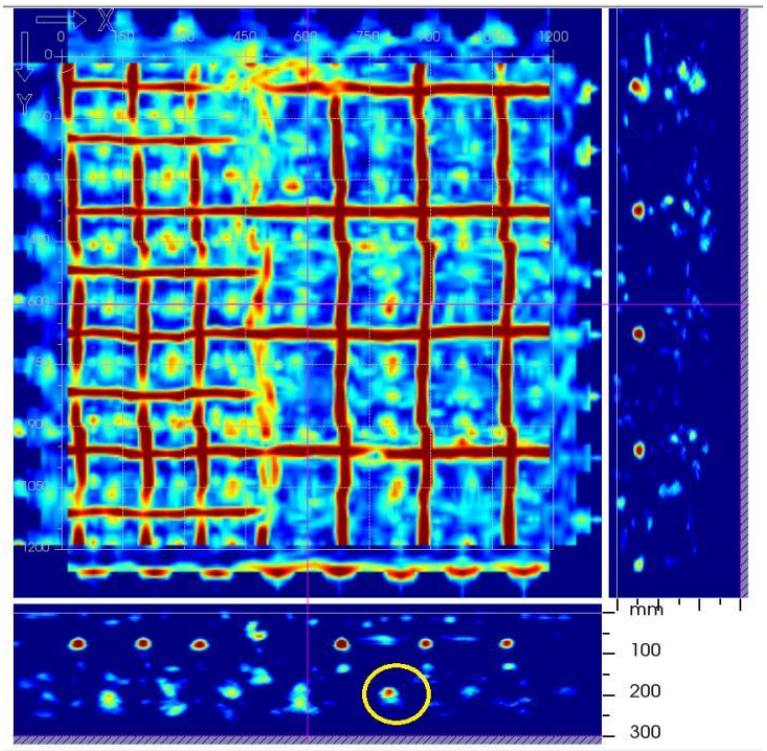

Figure 53 - Rebar Mapping and detection of anomalies form GPR 2nd scan of Side-B

From a 3D view of the scan, as shown in *Figure 54*, it is visible that rebars are not patterned as they are in the 1st scan of the Side-B of the wall.

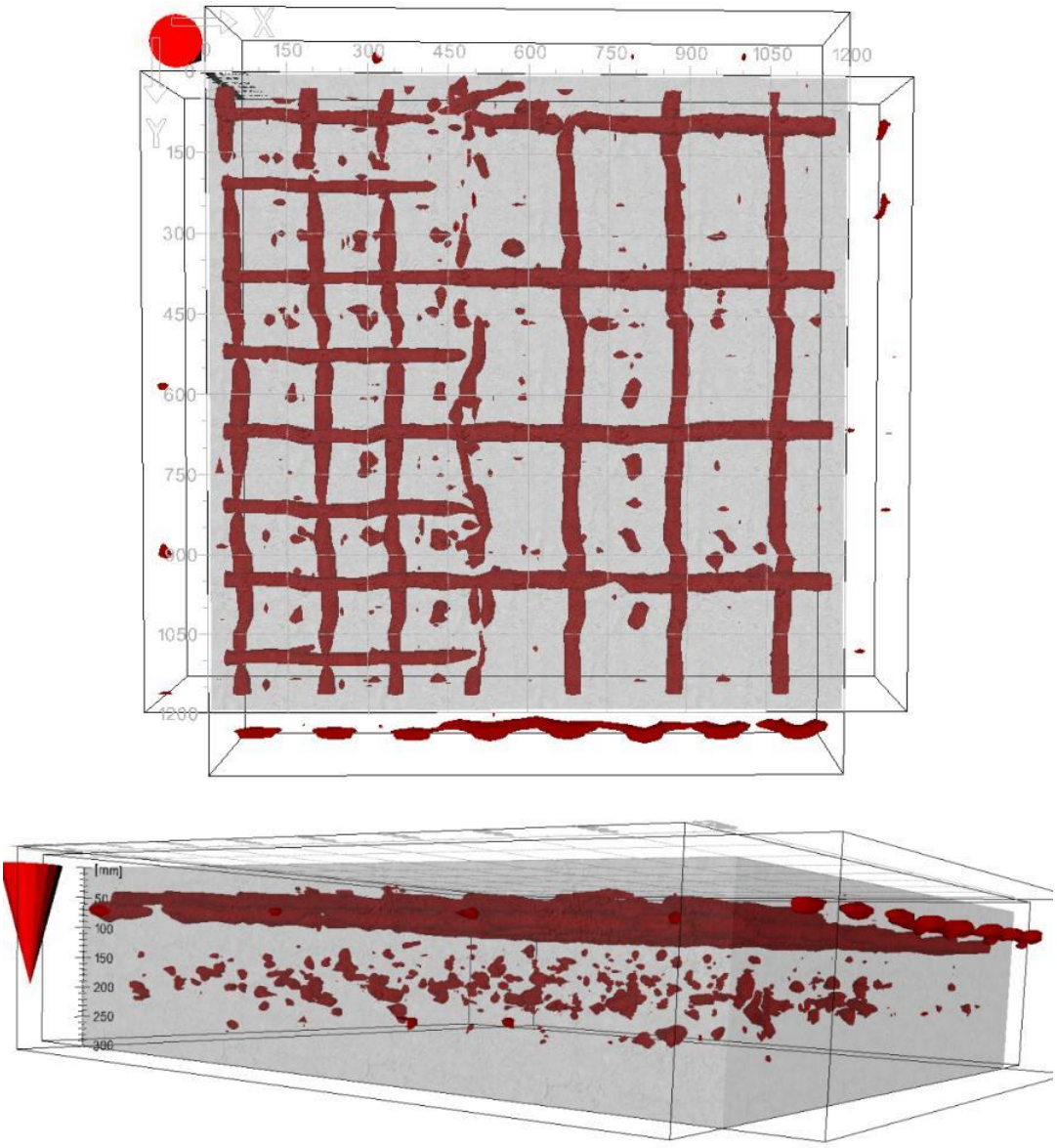

Figure 54-3D view of 2nd scan of Side -B showing the rebar details and other metallic object or voids

Side C

Figure 55 shows the 1st scan of the Side-C of the concrete wall having coordinates (0,0) (600,600), it gives the reinforcement location, and from the site, we can assume the concrete cover depth of the concrete wall. The location of reinforcement is 50mm from the top surface of the concrete wall, and it can be said that the concrete cover thickness is almost 50mm. From the scan, we can check how closely spaced the designed reinforcement of the wall is to the other sides of the wall.

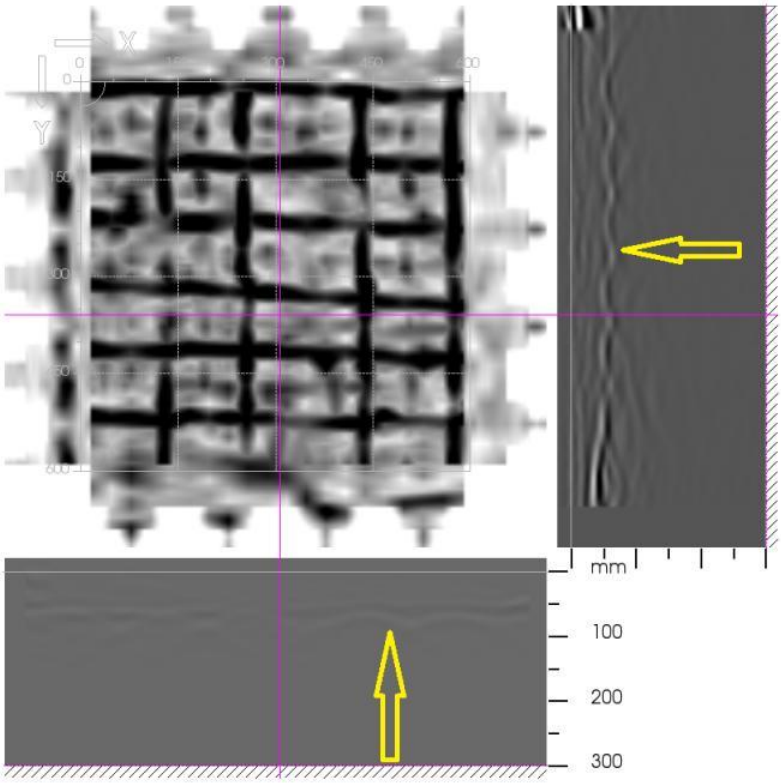

Figure 55 - Location of Rebars and Estimation of concrete cover depth using hyperbola curves from GPR 1st Scan of Side-C

Figure 56 reveals the reinforcement mapping and detection of different objects in the wall within a penetration depth of 300mm. Two objects are detected circled in the cross-sectional details of the scan. The rebar map is scattered and unable to define the different sizes of objects around the mesh. And objects are lying on the same level of reinforcement as shown from the 3D view of the scan. At 75mm from the top corner of the scan in the X direction, few objects are shown in the scan at the thickness range of 150 to 250mm of the cross-section as shown in the (). There are some voids and cracks in the surrounding rebars of this spectacular scanned area.

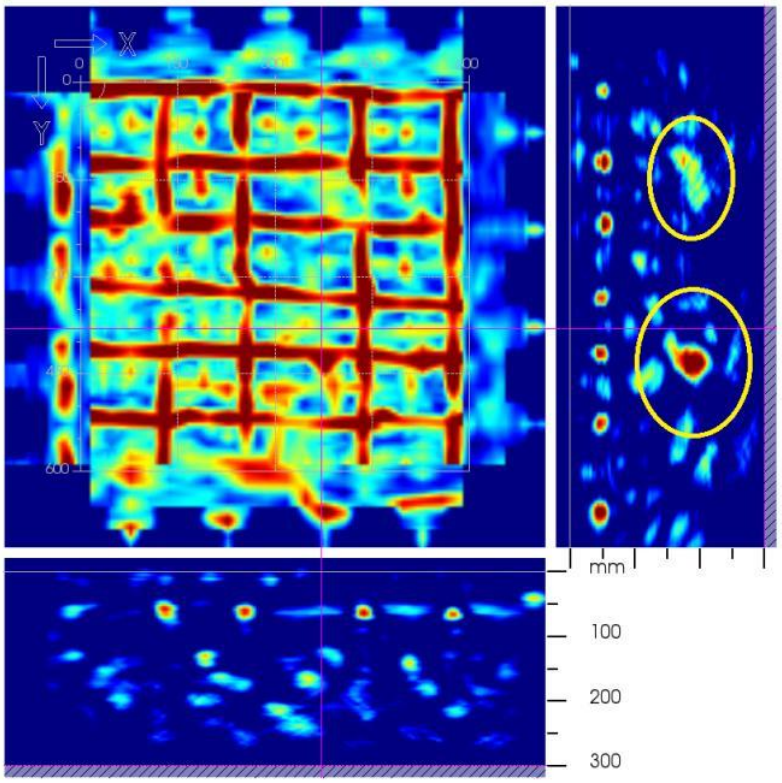

Figure 56 - Rebar Mapping and detection of anomalies form GPR 1st scan of Side-C

Figure 57 shows the 3D visualisation of the GPR scan obtained from Side C of the wall. Rebar mapping and different objects below the reinforcement map in the concrete subsurface are marked in this picture. These objects are voids, defects, or foreign objects it is hard to mention and impossible to clarify from the scans.

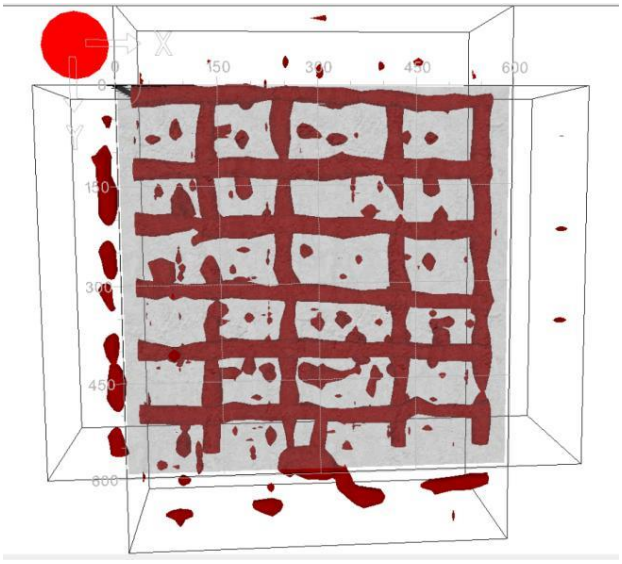

Figure 57 - 3D view of 1st scan of Side -C showing the rebar details and other metallic object or voids

*Figure 58*is 2nd scan of the wall side C, showing the location of the reinforcement, and *Figure 59* shows reinforcement mapping, and a few objects are

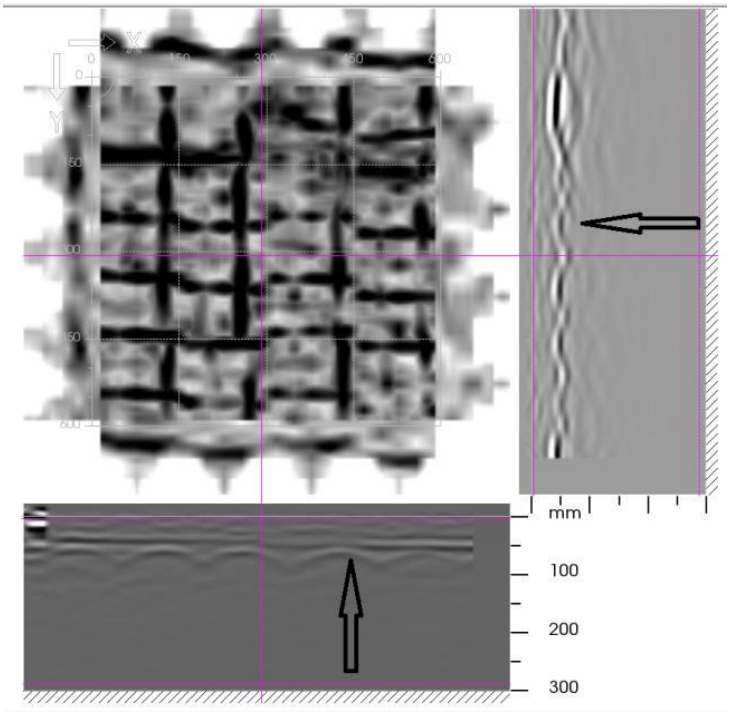

Figure 58 - Location of Rebars and Estimation of concrete cover depth using hyperbola curves from GPR 2nd Scan of Side-C

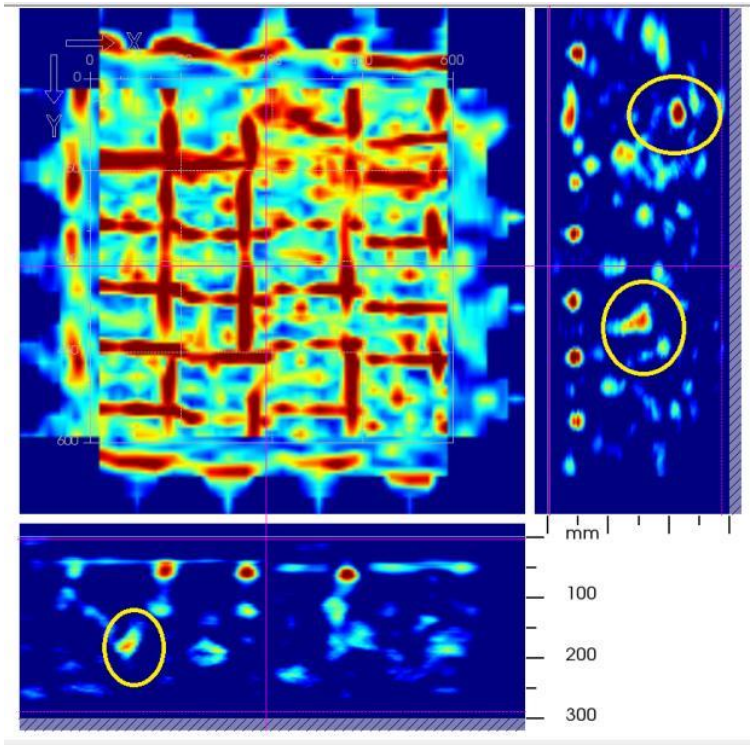

Figure 59 -Rebar Mapping and detection of anomalies form GPR 2nd scan of Side-C

They were detected by the GPR, as shown in the cross-sectional details of the scan. In the middle of the scan, rebars are shown broken or damaged.

Figure 60 describes the 3D view of the GPR scan. In the above picture, reinforcement and different objects are visible.

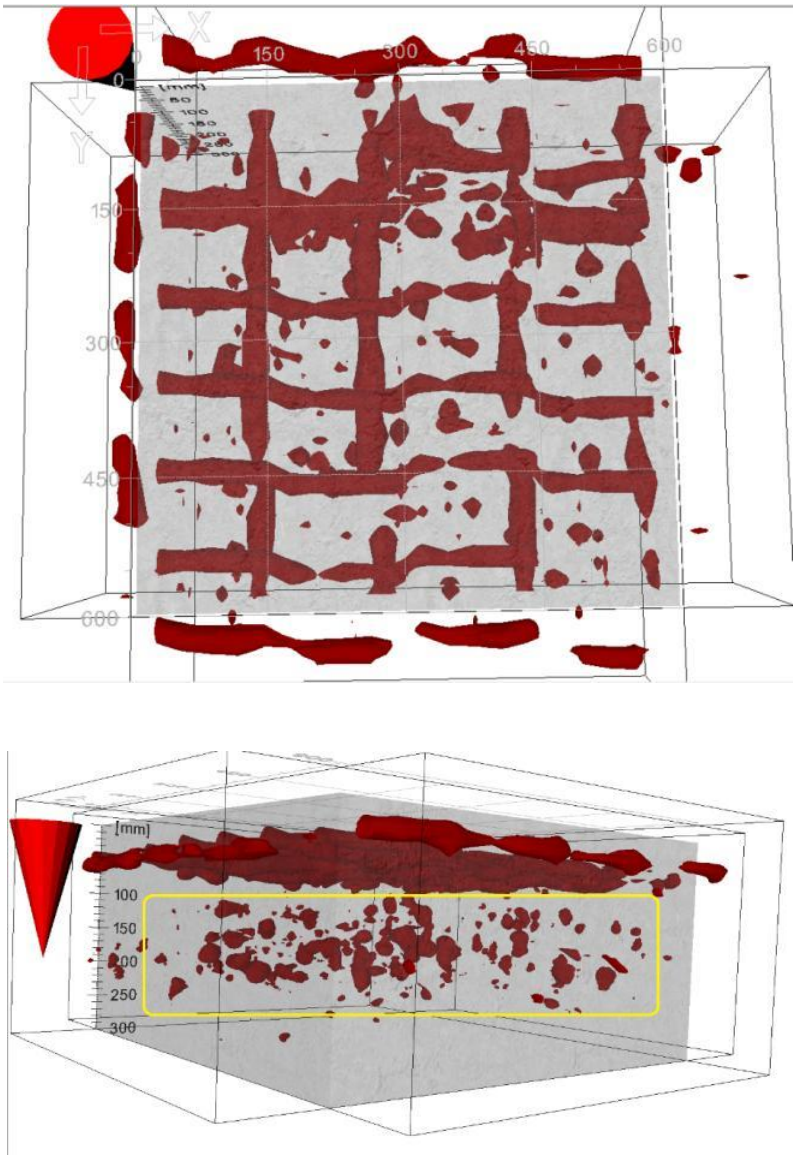

Figure 60 - 3D view of 2nd scan of Side -C showing the rebar details and other metallic object or voids

Floor

There are 20 scans obtained from the total area of the base of the wall from all sides, and scans are analysed. A few of them are described here, and other scans are in Appendix. GPR floor scans show reinforcement mapping, and using the dimensions of grid spacing; we assumed the rebar diameter and concrete cover thickness from the following scans. From all the scans, it is hard to define the detected objects except the reinforcement in the concrete wall and foundation of the wall, which is also referred to as the floor.

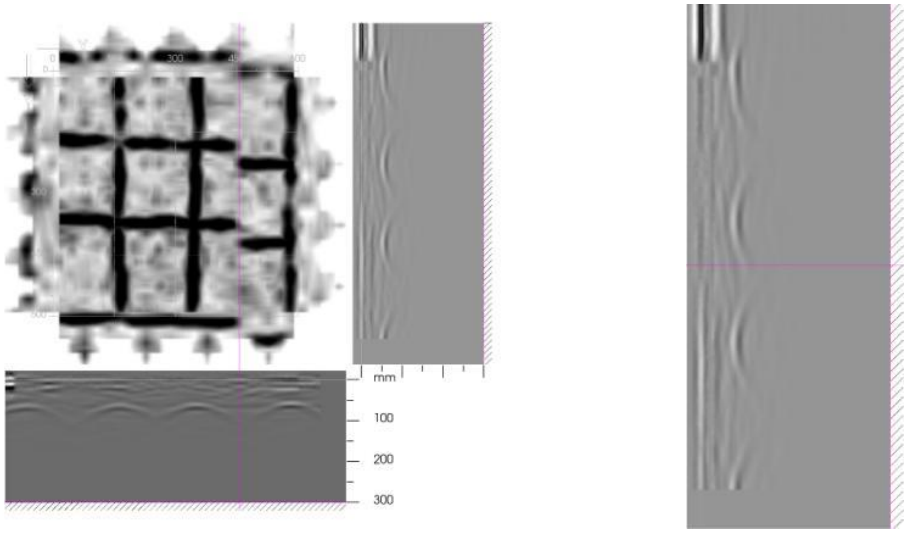

Figure 61- Location of Rebars and Estimation of concrete cover depth using hyperbola curves from GPR Scan of Floor

Figure 61 shows the location of the reinforcement on the floor of the wall; from the location of the reinforcement, the concrete cover is imagined, equal to 50mm.

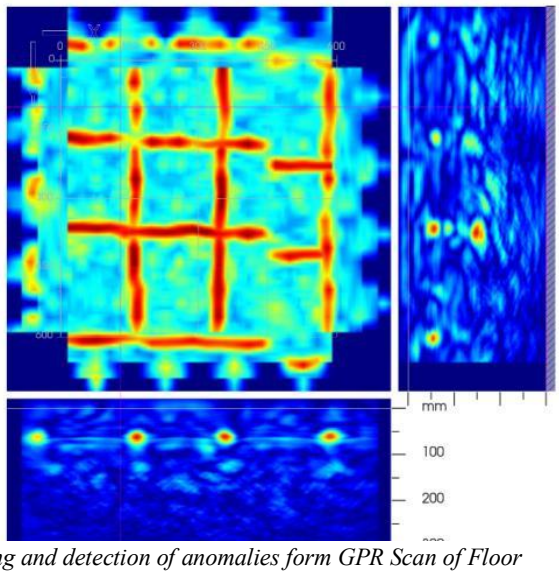

Figure 62 - Rebar Mapping and detection of anomalies form GPR Scan of Floor

Figure 62 reveals the reinforcement mapping and some detected objects shown in the cross-sectional details of the scan. Discontinuity in the rebar map at 450mm in X- direction is due to human error in the scanning process. Reinforcement spacing is about 150mm.

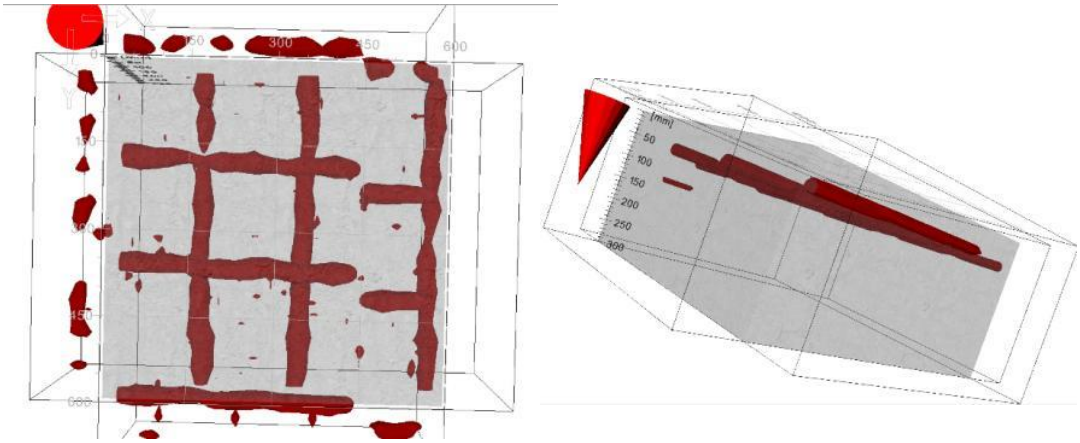

Figure 63 - 3D view of GPR scan of floor showing the rebar details and other metallic object or voids

Figure 63 shows the 3D visualisation of the GPR scan of the floor (Foundation of the concrete wall). From *Figure 63*, we can see the reinforcement detail, and in the 2nd part of the picture, there is a red line at a depth of 100mm. In the result of object smoothing of the scan, that line got visible, which means that there is a crack or a metal object at that location. Some foreign objects are also embedded in the concrete wall. That object could be one of those, but it is hard to define this spectacular object. Analysis of floor scans only provided information on reinforcement mapping, spacing between rebars and concrete cover of the bed. Rebar diameter is tentatively measured by keeping in view the grid spacing.

4.2 Investigation of reinforced concrete retaining wall

Figure 64 is the 1st scan of the concrete retaining wall and shows the location of the reinforcement in the retaining wall. From cross-sectional detail, the location of the rebars is approximately 150mm from the top of the concrete surface; it seems reinforcement is in the middle of the wall.

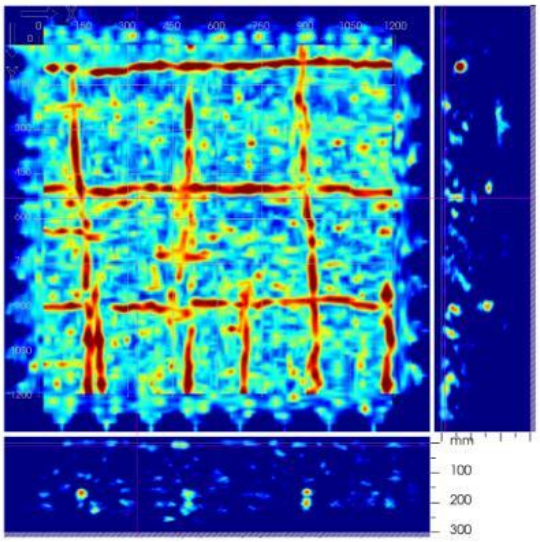

Figure 64 - Rebar mapping and detection of voids and anomalies in GPR Scan of Retaining Wall

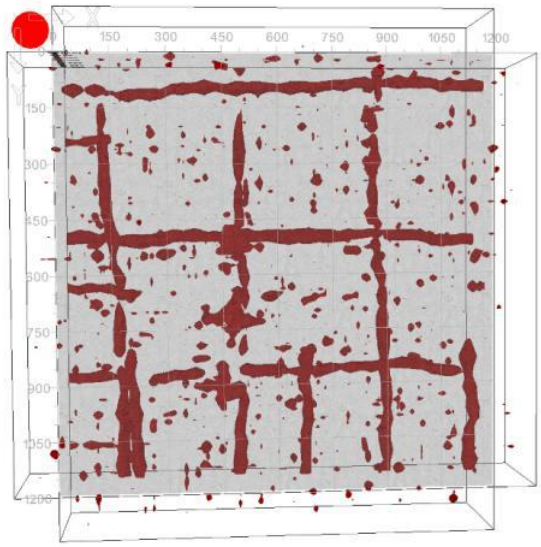

Figure 65 - 3D Visualization of GPR Scan of retaining wall

Figure 65 shows the exact location of reinforcement in the concrete retaining wall. From the 3D explanation of the wall scan, the wall thickness is 280mm,

as the last object detected shows at a depth of approximately 280mm. Two layers are shown in the scan, a layer at a depth of 50mm showing the smaller red-coloured objects, and these objects could be voided on the visible side of the wall. At the top of the scan, there is a red line going through the four scans of the wall at a depth of 50mm, showing a steel bar or crack on the top of the wall, as shown in *Figure 65*.

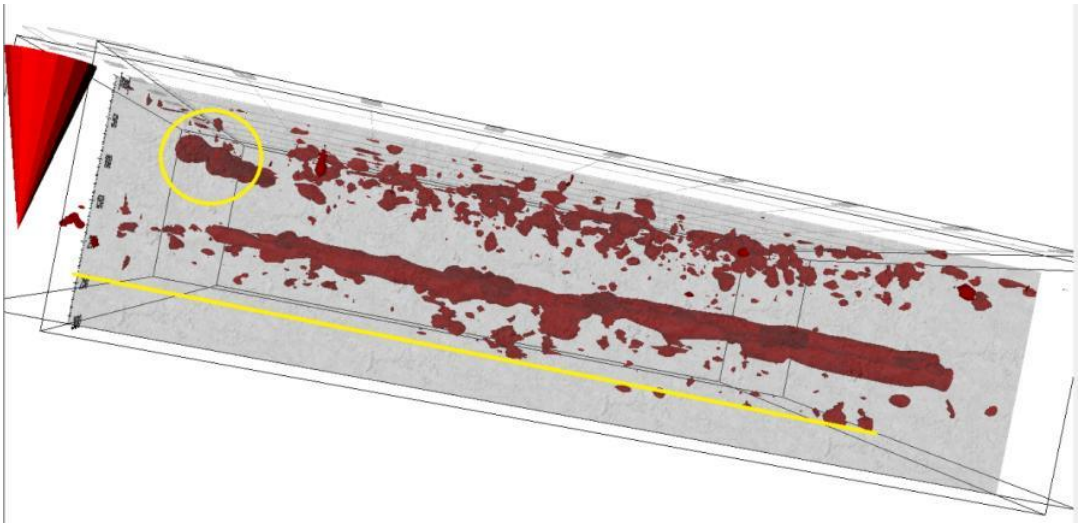

Figure 66 - 3D Visulization

Figure 66 shows the circled rebar that is rebar or cracks, it is unable to define at a depth of 50mm from the visible side of the wall, and the yellow line at the bottom shows the thickness level of the wall as the last object is detected at that depth of the scan. From *Figure 66*, it is clearly visible that the scan's reinforcement spacing and bottom stripe show that the six rebars and three bars are cut from the 300mm length, and the same scenario is at the left side of the scan. From the analysis of four scans of the wall, we came to know the retaining wall's reinforcement location and the wall's thickness.

4.3 Investigation of reinforced concrete slabs

Reinforced precast slabs are scanned, and three GPR scans are obtained from each slab.

Slab-1

Figure 67 shows the location of slab reinforcement as the deflected wave shown in the cross-sectional details. The scan location of reinforcement is between 50 to 75mm, and it depicts the concrete cover of the slab too. *Figure 68* talks about the slab thickness as when we move crosshairs to 200mm, we don't see any objects except the red object in the scan, which is supported under the slab at that location and showing here as the GPR penetration depth is 300mm. Yellow lines in the cross-sectional details show the thickness of the slab, which is almost equal to 200mm. In the cross-sectional details of *Figure 68*, it seems there is another rebar layer at the location of 150mm, which depicts that the reinforced precast slab is doubly reinforced or these are prestressed tendons, it is hard to say.

Figure 69 shows the premade holes in the slab, and we can see the depth of the holes from the cross-sectional details of the scan in the yellow boxes. Holes depth ends at 200mm, and the thickness of the slab can be evaluated to 200mm. The reinforced map is visible from all the scans, and the rebar diameter is measurable to 25mm. *Figure 70* explains the 3D visualisation of the GPR scan in which holes are clearly visible in the slab.

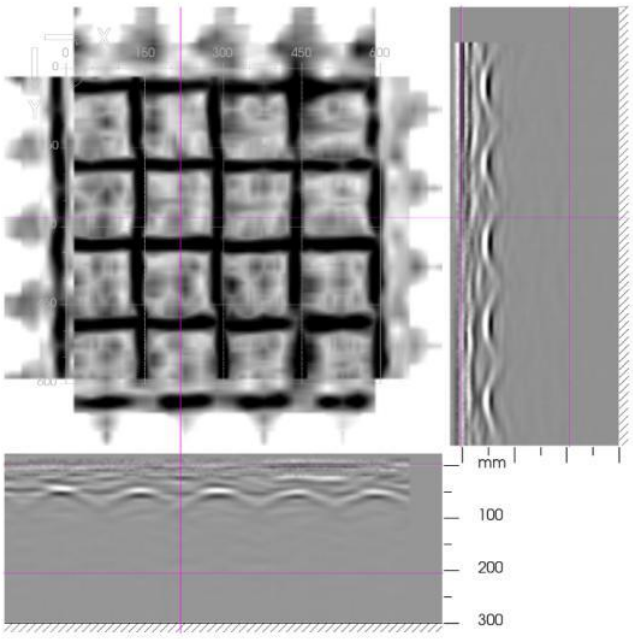

Figure 67 - Location of Rebars and Estimation of concrete cover depth using hyperbola curves from GPR Scan of Slab 1

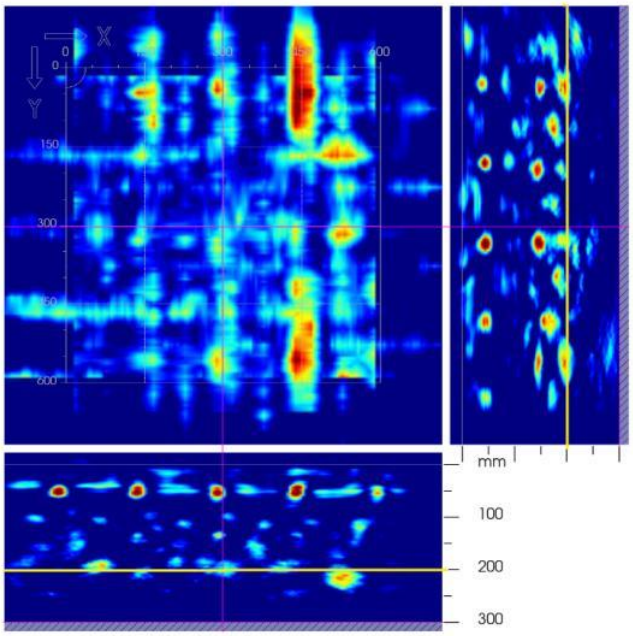

Figure 68 - Estimation of Slab thickness with cross hair movement

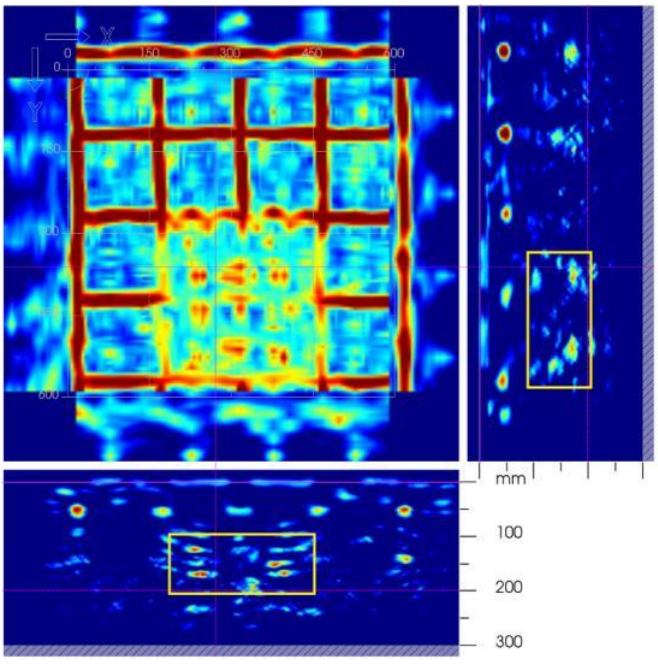

Figure 69 - Visualization of Holes in GPR Scan of Slab-1

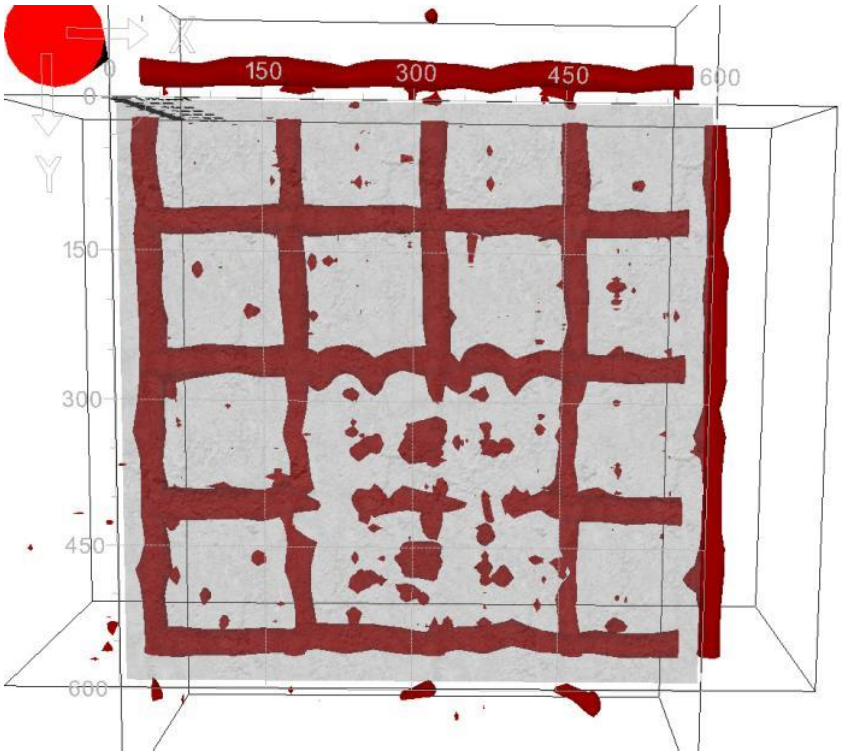

Figure 70 - 3D Visualization of GPR Scan of Slab -1

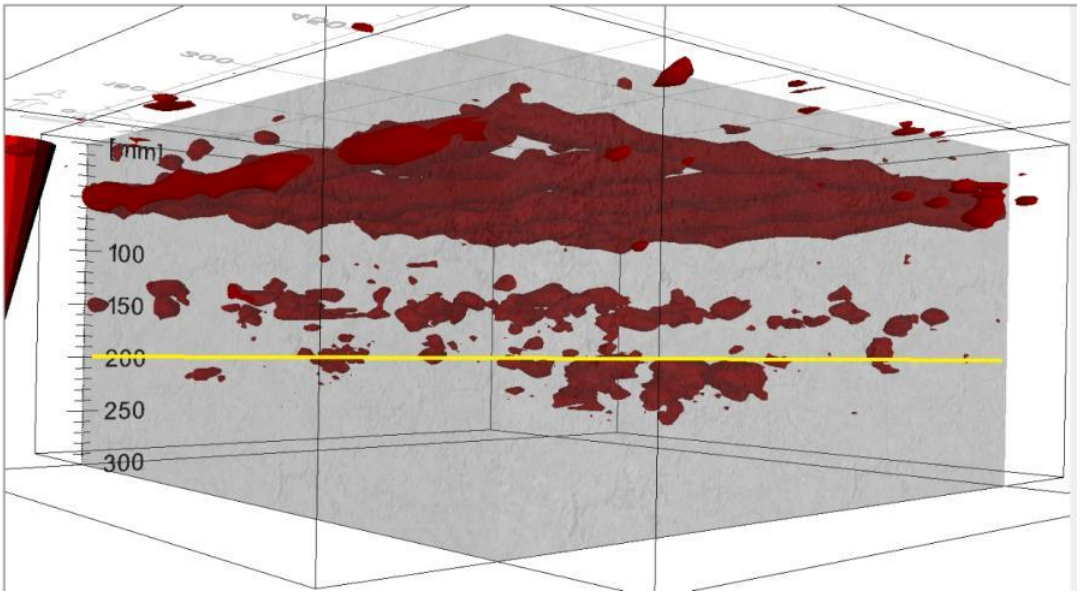

Figure 71 - Estimation of Thickness of precast slab

Slab-2

Figure 72 shows the GPR scan of the 2nd slab; from the scan, it is visible that when we move crosshairs to 200mm depth, there is nothing to see except the greenish particles, those are the concrete surface or soil surface below the concrete slab. Concrete slab thickness is measured and estimated as 200mm from the above scan, and at the location of 150mm deep from the top surface, there are objects shown as rebars, and those could be the prestressed tendons, or we can say that reinforced concrete slab is 200mm thick.

Figure 73 shows the detection of the rebar map, and the hole is clearly shown in the slab, as circled in the picture. In cross-sectional details, the dispersion of EM waves can be seen at the location of the hole. The diameter of the hole can be estimated as the dispersion of waves is confined between 150mm wide, shown in the scan. Hence the diameter of the hole can be assumed to be 150mm. In the third scan of the 2nd slab, three holes are at the top of the scan, and 3D details also prove the location of the holes. Other scans and details can be seen in Appendix.

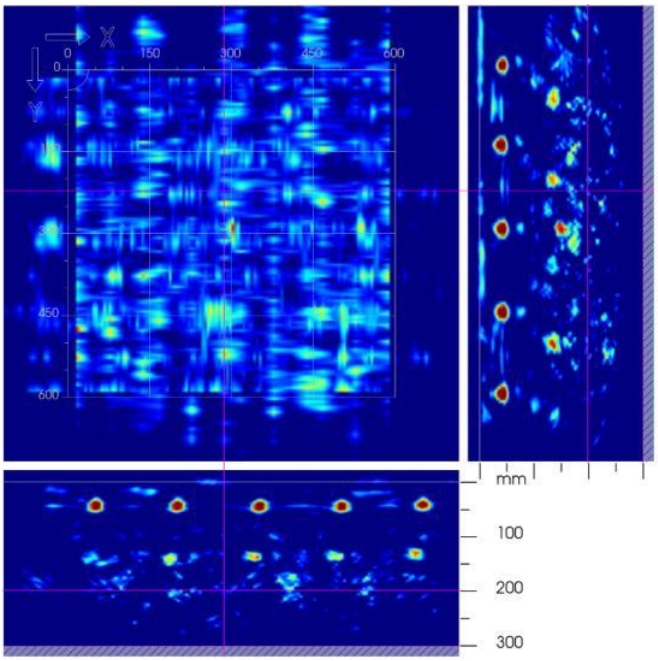

Figure 72 - Estimation of slab thickness

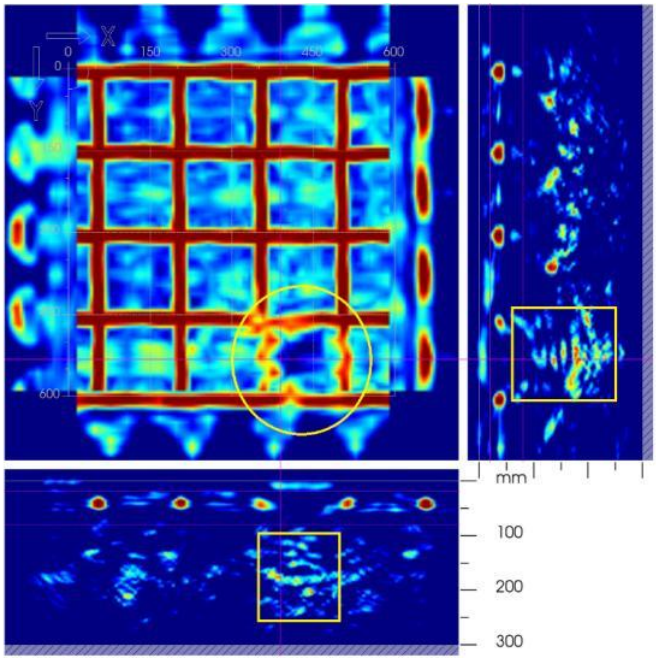

Figure 73 - Rebar mapping and hole detection of Slab -2

5 Summary and conclusion

This chapter concludes the thesis work, findings of the investigation of concrete structures using GPR, challenges and future research work recommendations.

5.1 Findings of the investigation

According to the objectives of this thesis work following are the results/ findings of the investigation:

- According to the analysis of GPR scans, detection of reinforcement, location, mapping and spacing can be checked and measured in the subsurface of concrete structures. Rebar spacing is measured from used reference grids for scanning purposes. In case of availability of the original design of concrete structure, reinforcement details can be cross-checked for structural capacity. In the case of doubly reinforced structures, only top reinforcement mapping is detectable using a GPR concrete scanner.
- Form hyperbolic curves in B-Scan concrete cover thickness can be estimated, as shown in *Figure 52*. The top of the hyperbolic cone gives the location of the rebar, and from the centre of the rebar to the top surface of the concrete, the concrete cover is calculated from the reference grid scale. Conrete cover thickness is estimated between 50 to 75 mm for scanned concrete structures in this thesis work except retaining wall, as shown in *Figure 64*, rebars are located at 200mm from the free side of the wall.
- From reinforcement mapping and 3D visualisation, rebar diameter is estimated using reference grid spacing. Most of the rebars are of 25mm diameter used in concrete structures under experiment for this thesis.
- From B-Scan analysis with crosshair movement, the depth of the concrete structure can be detected where no interruptions are seen in the scan, as seen in *Figure 72*. The thickness of precast slabs and retaining walls is estimated to be 200mm and retaining wall thickness is 280mm.
- Using PS-1000 X-Scan Concrete Scanner, metallic objects, voids, and construction defects are detected, but recognising these anomalies is difficult to form the scans and scan analysis. Construction defects (air voids/ honeycombs) are detectable, as shown in *Figure 58*, in cross-sectional detail hyperbolic profile is disturbed at the top, which indicates the presence of an air void or honeycomb in the thick concrete faux wall.

- Reinforcement defects are found, like irregular spacing and rebar breakage (corroded/ rusted), as shown in *Figure 64*.
- Foreign objects like electrical wiring, prestressed tendons and other simulated defects are detected in GPR scans. *Figure 48* and *Figure 66* provide the details of hidden objects except for reinforcement in the concrete subsurface. In this thesis work, simulated defects and internal cracks are not recognised from the analysis of GPOR scans.
- A difference is observed during the analysis of the scan between scaling depths 3 and 12. By changing the rising depth o from 3 to 12 and the offset location was put to 0, the reinforcement location is observed to come closer to the top surface, as shown in *Figure 74* & *Figure 75*. In *Figure 74* depth scale is three, and the reinforcement location is at 125mm, while in *Figure 75* location of reinforcement is at 50mm. It is also shown from the comparison that the visibility of reinforcement is much clearer using the 12-depth scale than the depth scale at 3. For analysis purposes of the GPR scans, we used a depth scaling of 12.

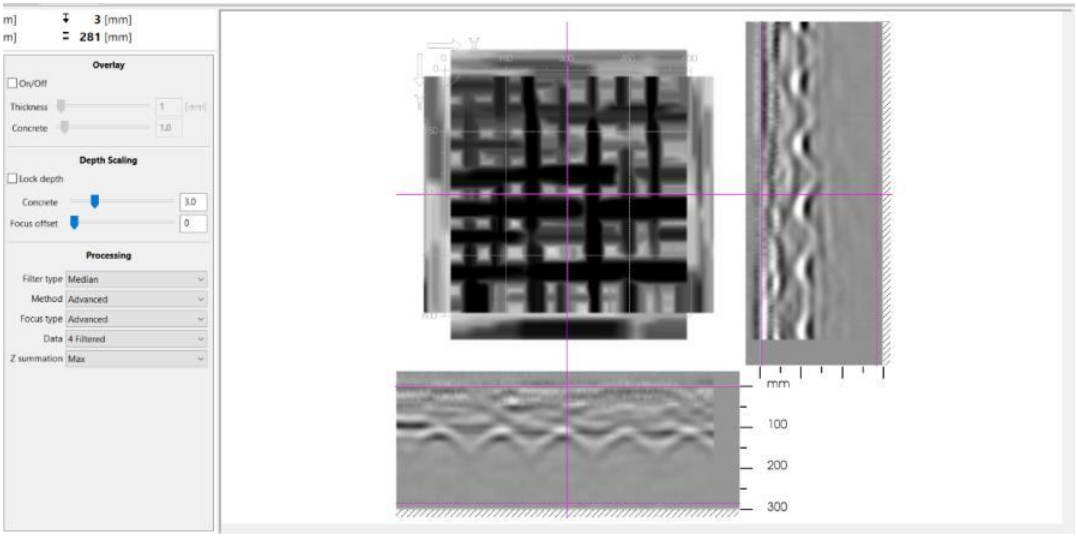

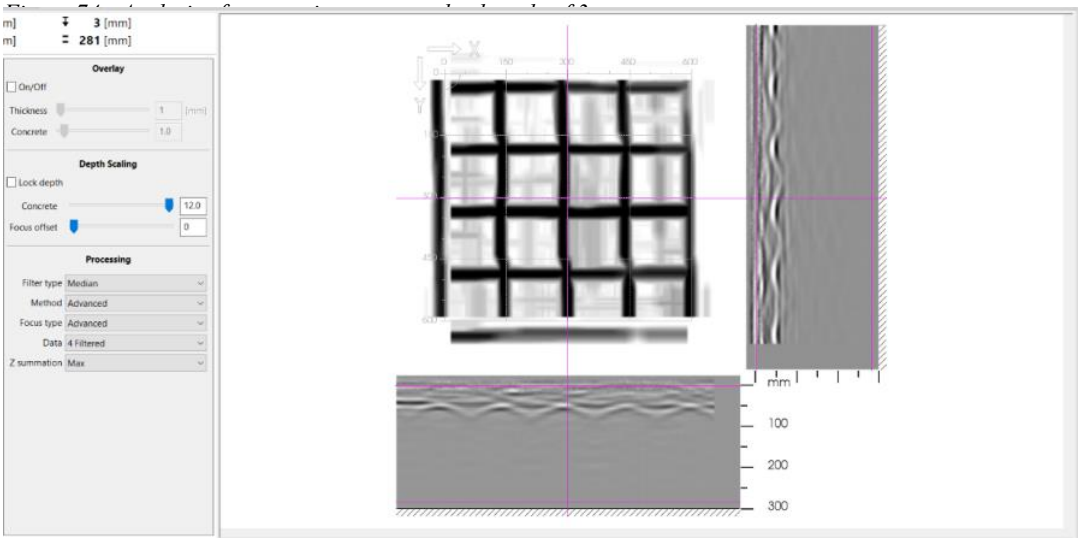

Figure 75 - Scan Analysis with depth scale 12 in Profis Detection Software

5.2 Challenges of the investigation

Due to the penetration depth of 300mm, we cannot see the whole depth of the thick concrete wall as some foreign objects are embedded in the wall. We need help finding the exact location and identification of the detected objects. The software used for the analysis of the GPR scans needs to be updated, and unable to measure the rebar diameter using extra functions in the latest update Profis Detection. This is done to evaluate the scans and get effective results as possible. Due to the unavailability of the original design of the concrete wall, retaining wall and precast slabs, we can't cross-check the detected objects with original design.

5.3 Future Research Recommendations

- PS-1000 X-Scan Concrete Scanner can be used for detection of hidden objects in concrete structures, and detailed information about hidden objects is possible with update of analysis software (Profis Detection Software), especially in future update diameter of rebar and size of hidden objects is able to determine.

6 References

Ahmed, Z. A. (2018). Effect of freezing-thawing on concrete behavior. *Challenge Journal of Concrete Research Letters*.

ALI M. SOHI, S. S. (2020). INFLUENCE OF VOIDS' SIZES AND LOCATIONS ON THE CONCRETE COMPRESSIVE STRENGTH.

Anthony D. Rosato, D. L. (2001). A perspective on vibration-induced size segregation of granular materials. *Chemical Engineering Sciences 57*.

BASHIR ALAM, M. A. (n.d.). Sulphate Attack in High-Performance Concrete-A Review. *International Journal of Advanced Structures and Geotechnical Engineering*.

Chemrouk, M. (n.d.). The deterioration of reinforced concrete and the option of high-performance reinforced concrete. *The 5th International Conference of Euro Asia Civil Engineering Forum (EACEF-5)*.

Creegan, P. J. (1998). Erosion of Concrete in Hydraulic Structures. *ACI Report* .

Dorner, R. E. (n.d.). Modelling acid attack on concrete: Part I. The essential mechanisms. *Science Direct* .

Dyer, M. J. (2019). *Lea's Chemistry of Cement and Concrete*.

Fabio Tosti, V. G. (2019). Transport infrastructure monitoring by data fusion of GPR and SAR imagery information. *Transportation Research Procedia 45*.

Faheem Al-Neshawy, T. O. (2018). Mock-up wall for non-destructive testing and evaluation of thick reinforced concrete structures in nuclear power plants.

Farshad Rajabipour, E. G. (n.d.). Alkali–silica reaction: Current understanding of the reaction mechanisms and the knowledge gaps. *Cement and Concrete Research*.

H. Sezer Atamturktur, C. R. (n.d.). Detection of Internal Defects in Concrete Members Using. *Detection of Internal Defects in Concrete Members Using*.

Henrique Lorenzo, M. H. (2000). In-situ radar remote sensing applied to detect degradation in a concrete floor.

HILTI. (n.d.). *Operating-Instruction-PS-1000-01-EN-Operating-Instruction-PUB-5310653-000.pdf*.

J. Rhazi, O. D. (n.d.). DETECTION OF FRACTURES IN CONCRETE BY THE GPR TECHNIQUE.

J. Rhazi, O. D. (n.d.). DETECTION OF FRACTURES IN CONCRETE BY THE GPR TECHNIQUE.

John Newman, B. S. (2003). *Advanced Concrete Technology 2- Concrete Properties*.

K. Agred, G. K.-P. (2018). The reinforcement and moisture assessment location is reinforced concrete with a double receiver GPR antenna.

Larbi, T. N. (2010). *Non-Destructive Evaluation of Reinforced Concrete Structures: Deterioration Processes and Standard Test Methods*.

Lasse Petersen, L. L. (July-August 2007). Influence of Freezing-and-Thawing Damage on Behavior of Reinforced Concrete Elements. *ACI MATERIALS JOURNAL*.

Leading. (n.d.). Retrieved November 29, 2019, from Wikipedia: https://en.wikipedia.org/wiki/Leading

Line length. (n.d.). Retrieved November 29, 2019, from Wikipedia: https://en.wikipedia.org/wiki/Line_length

M. Salucci, L. P. (2016). Advanced multi-frequency GPR data processing for non-linear deterministic imaging. *Signal Processing* .

M.G. Hernandez, M. I. (2000). Porosity estimation of concrete by ultrasonic NDE.

Mastrangelo, J. H. (2006). GPR inspection of concrete bridges. *Science Direct* .

Mezgeen A. Rasol, V. P.-G. (2020). GPR laboratory tests and numerical models to characterize cracks in cement concrete specimens, exemplifying damage in rigid pavement. *Measurement* .

Miss. Neha.V.Bagdiya, P. S. (n.d.). Review Paper on Construction Defects. *Review Paper on Construction Defects*.

Mr. Jaydeep D. Agola, M. B. (n.d.). CONCEPTUAL STUDY ON CONSTRUCTION DEFECTS AND ITS SOLUTION . *IJARESM*.

Naotoshi YasudaNorikazu, M. &. (2020). Detection and characteristics estimation of defects in concrete structures using laser ablation-induced vibration.

Neshawy, F. A. (n.d.). Deradation Mechanisms of Concrete .

Nuria Forcada, M. M. (2014). Assessment of construction defects in residential buildings in Spain.

Pajewski, A. B. (2015). Civil Engineering Applications of Ground Penetrating Radar . In A. B. Pajewski (Ed.), *Civil Engineering Applications of Ground Penetrating Radar* . Springer .

Penttala, V. (n.d.). *Causes and mechanisms of deterioration in* .

Penttala, V. (n.d.). Causes and mechanisms of deterioration in reinforced concrete.

Pooja Nama, A. J. (n.d.). Study on Causes of Cracks & its Preventive Measures in Concrete . *Study on Causes of Cracks & its Preventive Measures in Concrete* .

Products, H. (n.d.). *Operating Instructions PS-1000-01*. HILTI.

Riaan Combrinck, L. S. (n.d.). Interaction between settlement and shrinkage cracking in plastic. *Interaction between settlement and shrinkage cracking in plastic*.

Ruoyu Chen, K. T. (2021). Detection of delamination and rebar debonding in concrete structures with ultrasonic SH-waveform tomography. *Automation in Construction*.

Ruoyu Chen, K. T. (2022). Detection of delamination and rebar debonding in concrete structures with ultrasonic SH-waveform tomography. *Automation in Constrcution* .

S. Laurens, J. B. (2005). Non-destructive evaluation of concrete moisture by GPR: experimental study and direct modeling . *Materials and Structures 38*.

Safiuddin, B. D. (n.d.). Abrasion Resistance of Concrete – Design, Construction and Case Study . *Concrete Research* .

Sai Teja Kuchipudi, D. G. (2022). Detection of Debonds in Reinforced Concrete Using Ground Penetrating Radar.

Saraswathy, H.-W. S. (2007). Corrosion Monitoring of Reinforced Concrete Structures - A Review .

Schutter, G. D. (2013). *Damage to Concrete Structures* . CRC Press .

Senlin Yang, Z. W. (2021). Defect segmentation: Mapping tunnel lining internal defects with ground penetrating radar data using a convolutional neural network.

Tahar Bachiri, M. H. (2022). Examinating GPR based detection of defects in RC builds .

Tess X.H. Luo, W. W. (2019). GPR imaging criteria. *Journal of Applied Geophysics*.

Tsang, W. L. (2006). Characterization of pore systems of air/water-cured concrete using ground penetrating radar (GPR) through continuous water injection. *COnstruction and Building Materials 22*.

Uno, P. J. (1998). Plastic Shrinkage Cracking and Evaporation Formulas. *ACI Materials Journal*.

Vega Pérez-Gracia, D. D.-D. (2009). Laboratory characterisation of a GPR antenna for high-resolution testing: radiation pattern and vertical resolution. *NDT & E International* (Elsevier).

Visual elements. (n.d.). Retrieved November 29, 2019, from Aalto University brand library: https://www.aalto.fi/en/visual-library#/visual-elements/typography

W.L. Lai, S. K. (2009). Characterization of concrete properties from dielectric properties using ground penetrating radar. *Cement and Concrete Research*.

W.L. Lai, T. K. (2010). Using ground penetrating radar and time–frequency analysis to characterise construction materials. *NDT & E International* .

Xiongyao Xie, P. L. (2013). GPR identification of voids inside concrete based on the support vector machine algorithm.

Y. Zhou, B. G. (n.d.). Carbonation-Induced and Chloride-Induced Corrosion in Reinforced Concrete Structures.

Yelf, R. J. (2007). Application of Ground Penetrating Radar to Civil and Geotechnical Engineering.

Yelf, R. J. (2015). Application of Ground Penetrating Radar to Civil and Geotechnical Engineering.
Yelf, R. J. (2015). Application of Ground Penetrating Radar to Civil and Geotechnical Engineering.
Zhou, Y. (n.d.). Carbonation-Induced and Chloride-Induced Corrosion in Reinforced Concrete Structures. *American Society of Civil Engineers*.